

SKB

**TECHNICAL
REPORT**

86-25

**Aspects of the Physical State of
Smectite-adsorbed Water**

Roland Pusch, Ola Karnland
Swedish Geological Co, Lund
Engineering Geology

December 1986

ASPECTS OF THE PHYSICAL STATE OF SMECTITE-ADSORBED
WATER

Roland Pusch, Ola Karnland
Swedish Geological Co, Lund

December 1986

This report concerns a study which was conducted for SKB. The conclusions and viewpoints presented in the report are those of the author(s) and do not necessarily coincide with those of the client.

A list of other reports published in this series during 1986 is attached at the end of this report. Information on KBS technical reports from 1977-1978 (TR 121), 1979 (TR 79-28), 1980 (TR 80-26), 1981 (TR 81-17), 1982 (TR 82-28), 1983 (TR 83-77), 1984 (TR 85-01) and 1985 (TR 85-20) is available through SKB.

SWEDISH GEOLOGICAL CO
Roland Pusch/JS

Date: 1986-12-31
ID-no: IRAP 86524

ASPECTS OF THE PHYSICAL STATE
OF SMECTITE-ADSORBED WATER

Roland Pusch
Ola Karnland

Swedish Geological Co, Lund
Engineering Geology
December 1986

Key words: porewater density, dilatometry, electron diffractometry,
high-voltage electron microscopy, microstructure, montmo-
rillonite, smectite

CONTENTS

	Page
SUMMARY	I
1 INTRODUCTION	2
2 CONSTITUTION OF WATER SATURATED MONTMORILLONITE CLAY	2
2.1 General	2
2.2 The mineral montmorillonite	3
2.2.1 Crystal structure	3
2.2.2 Shape and size of smectite crystals	4
2.2.3 Microstructure	5
2.3 Pore water, internal and external water	9
2.3.1 General	9
2.3.2 Quantitative microstructural analysis	10
2.3.3 Conclusions	14
3 CLAY-WATER INTERACTIONS	15
3.1 Current concepts of smectite-adsorbed water	15
3.1.1 Recent literature review	15
3.1.2 The Forslind concept	19
3.1.3 Energy considerations	22
3.1.4 The porewater density	24
3.2 Conclusions	27
4 EXPERIMENTAL	28
4.1 Test philosophy	28
4.2 The hydration process in Na montmorillonite and the associated microstructural evolution	29
4.2.1 HVEM-microscopy	29
4.2.2 Electron diffractometry	33
4.2.2.1 Orientation of crystal flakes in stacks	33
4.2.2.2 Electron diffraction of hydrating montmorillonite	33
4.3 Dilatometer tests	35
4.3.1 Test technique	35
4.3.1.1 Pilot tests	35

4.3.1.2	Main tests	36
4.3.2	Clay material	36
4.3.3	Preparation of clay samples	38
4.3.4	The pycnometer device	39
4.3.5	Test program	41
4.3.6	Test results	41
4.3.6.1	General	41
4.3.6.2	Distilled water	42
4.3.6.3	CaCl ₂ solution	44
4.4	Discussion	46
4.4.1	General	46
4.4.2	Accuracy	46
4.4.3	Influence of the ratio of internal and external water	47
4.4.4	Influence of exchange from Na to Ca	50
5	CONCLUSIONS	51
6	RECOMMENDATIONS FOR FURTHER WORK	55
7	ACKNOWLEDGEMENTS	56
8	REFERENCES	57

SUMMARY

The hydration of Na montmorillonite is currently explained in two ways, which are related to different crystal structure versions of this mineral. Wetting of the Edelman/Favejee structure takes place through formation of an ice-like hydrogen-bonded water lattice that grows from assumed, protruding hydroxyls in the basal planes, yielding interlamellar water of a density well below 1 g/cm^3 . The hydration of the conventional Hofmann/Endell/Wilm structure instead implies that interlamellar cations hydrate and that the spatial arrangement of the water therefore depends on the location of positive clay lattice charge. The molecular arrangement may thus vary and yield a density of the interlamellar water that may be lower, equal to, or higher than that of free water.

The amount of interlamellar water depends on the microstructure of the clay. At bulk densities exceeding $1.6\text{-}1.8 \text{ t/m}^3$ it constitutes 40-80 % of the total porewater content, while at densities lower than about 1.3 t/m^3 this percentage drops to less than 5.

One way of finding out which of the two hydrate models that is valid at room temperature would be to determine the density of interlamellar water. Reinterpretation of published data and the outcome of recent experiments using dilatometer technique all point to an average density of such water of slightly more than 0.9 g/cm^3 , which suggests that ice-like water lattices are formed in the interlamellar space when Li and Na are adsorbed cations. External surfaces of stacks of montmorillonite flakes are concluded to have a negligible ordering influence on the porewater, which therefore has a density on the same order as free water.

1 INTRODUCTION

The rather extreme water-sealing properties of smectite-rich clays as well as their swelling potential and strong affinity for water have long been assumed to result from physico/chemical interaction between the crystal lattice of such minerals and water molecules. Various laboratory investigations of the bulk properties of such clays indicate that this interaction may be very strong, the most striking example being that smectite clays with a water content of 20-40 % by weight exhibit a high shear strength and very moderate creep strain rates despite the fact that water separates all the crystallites. This suggests that the intercrystalline water is in a physical state which is quite different from that of free water.

Physical and mathematical modelling of the processes that are involved in water and gas percolation, shear, creep and swelling, require a much improved understanding of the physical constitution of the water in smectite clays. This report, which adds some new information to the presently available literature data, is an attempt to form a base for derivation of a general physical clay/water model for montmorillonite. In particular, it is focussed on the importance of the distribution of strongly mineral-influenced porewater. Dilatometer measurements are reported which serve to illustrate the relevance of currently favored water structures in montmorillonite clay of low and high density and with Na or Ca as adsorbed cation.

2 CONSTITUTION OF WATER SATURATED MONTMORILLONITE CLAY

2.1 General

Montmorillonite crystals are known to interact strongly with the first few hydrate layers and since the specific surface area is very large, i.e. 600-800 m²/g in the sodium state, a major part of the water in dense montmorillonite clay is assumed to be in a physical state that is different from that of free water. Since there is supposed to be a decay in interaction at increasing distance from

the basal planes of the crystals there is a strong need to quantify the interparticle distance for interpretation of the physical state of the "porewater" from various bulk clay tests. This matter is of vital importance as demonstrated in the report.

2.2 The mineral montmorillonite

2.2.1 Crystal structure

There are two possible theoretical crystal lattice models for montmorillonite, i.e. the Hofmann/Endell/Wilm (HEW) version and the one suggested by Edelman and Favejee (EF). They are represented by the compositions in Eqs (1) and (2) and the atomic arrangements shown in Fig 1. XRD or chemical analyses cannot be used to distinguish between them and both will be referred to in the subsequent text since it is presently not known which model that applies and since their atom lattice configurations may influence the physical state of part of the porewater in different ways.

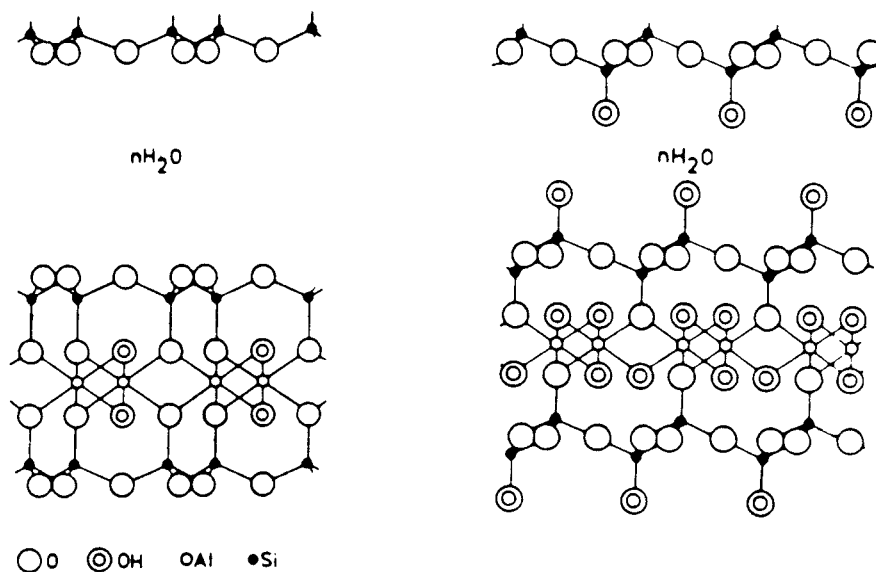
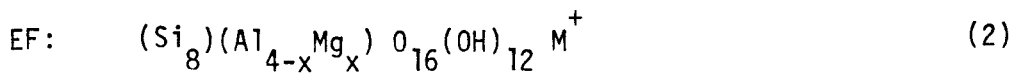
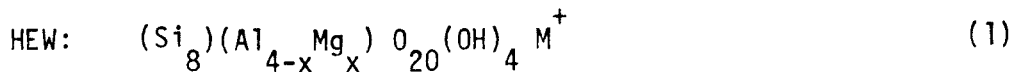


Fig 1. The montmorillonite crystal lattice. Left: The HEW structure. Right: The EF structure



The EF model deviates from the traditionally favored HEW structure with respect to the type of coordination of the tetrahedra, which have been termed trans- for the EF structure and cis- for the HEW version. We see that every second tetrahedron of the silicious sheets is inverted, thus exposing apical OH:s which absorb water through hydrogen bonding and which can also exchange the proton. Since only about 20 % of the cation exchange capacity appears to be due to such place exchange, the model has later been adjusted to one with a smaller number of inverted tetrahedrons although this correction may not be required as discussed in a subsequent section (1).

As to the crystallographic conditions it should be noticed that both versions are usually claimed to be monoclinic as is also the basic form of pyrophyllite with only Al in octahedral positions. While the latter mineral has no net lattice charge and no water molecules between the layers, montmorillonite of the HEW type is assumed to have vacancies and octahedral as well as tetrahedral substitutions that yield a net negative lattice charge and interlamellar uptake of cations. This is in contrast with the EF structure, which in its theoretical, perfect form gains its cation exchange properties through proton dissociation from the protruding OH-groups. Electron diffraction spot patterns usually show hexagonal symmetry instead of the expected two-fold, which has been explained by bending of flakes with tetrahedral oxygens (or OH:s) rotated from their positions by a plausible amount (2). Also, it has been stated that in thicker aggregates the aligned flakes (e.g. domains) are stacked with mutual rotations around the perpendicular to their plane. These observations indicate that the degree of ordering may be relatively low in larger stacks, which has a bearing on the microstructural (fabric) constitution as well as on the physical state of intercalated water.

2.2.2 Shape and size of smectite crystals

It appears from various electron microscope studies that effectively dispersed smectite clays consist of individual razorblade-shaped

lamellae with a maximum diameter that ranges between about 0.05 and 0.5 μm (Fig 2). Usually, they exhibit twisted, bent and even curled forms.

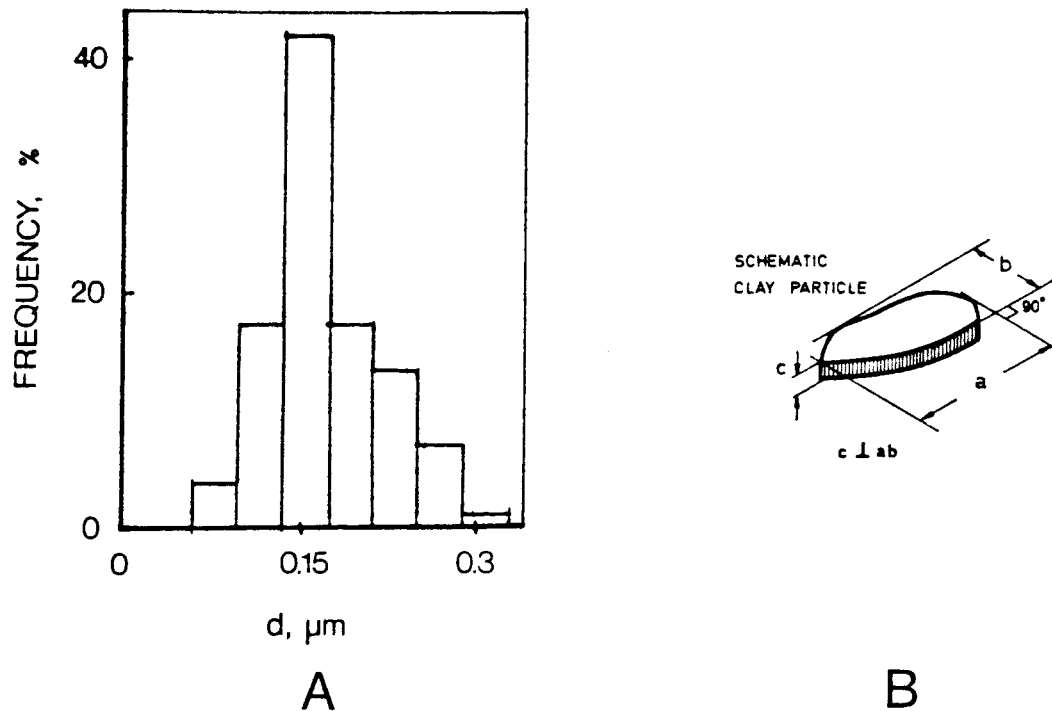


Fig 2. Example of smectite particle size distribution. A) Distribution based on the Stoke diameter (d). B) Definition of particle size and shape; d can roughly be taken as the average of a , b and c (4)

2.2.3 Microstructure

The problem of identifying the detailed particle arrangement in expandable smectite clays without producing artefacts was recognized a couple of decades ago when rather intense work was conducted to develop techniques for microstructural investigations using electron microscopy (5). Since then, two main methods have been applied, one being mechanical fracturing of freeze-dried specimens for scanning electron microscopy after gold-coating, the other being transmission electron microscopy of ultrathin microtome-cut sections after replacement of the pore fluid by a suitable resin.

Freezing, however rapidly made, is known to affect the particle arrangement. It leads to a rapid expulsion of intercrystalline water

associated with a shrinkage of clay crystal aggregates that consist of aligned, parallel crystal lamellae. After freezing the interlamellar space hosts one to two monolayers of water molecules (4), which means that if the actual arrangement is that of crystallites separated by more than two hydrate layers, freezing will contract the particle aggregates and enlarge interaggregate pores through the accumulation of ice in them (Figs 3 and 4).

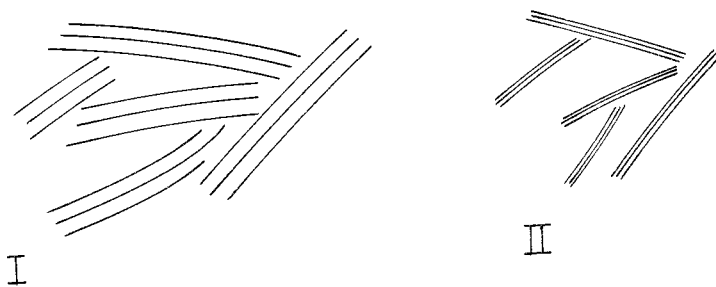


Fig 3. Schematic picture of structural rearrangement caused by freeze-drying of montmorillonite. I) Original state, II) freeze-dried state

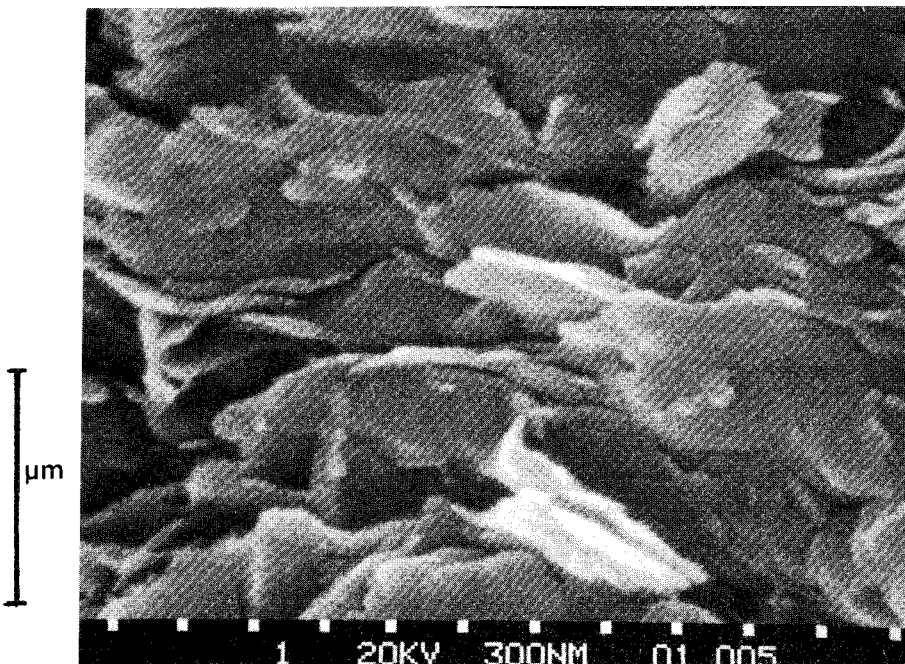


Fig 4. Scanning electron micrograph of montmorillonite-rich bentonite from 300 m depth in Gotland

Fig 4 is a representative scanning micrograph of a freeze-dried very dense smectite clay, the obvious degree of particle orientation being caused by the high overburden pressure (3.5 MPa). The pores seen in the micrograph are probably considerably wider than in the original state, while the domain-type particles are more condensed than in nature. Thus, each particle consists of dense groupings of several tens of smectite lamellae with a wider spacing in the natural state.

Several resin preparation techniques are known to yield large expansion of dense smectites if they are free to swell, while soft clays of this sort are assumed to be very little affected by such treatment. If the sample is confined throughout the preparation as well as in the polymerization phase, the microstructural pattern is expected to be largely preserved regardless of the density. Transmission electron microscopy of ultrathin sections obtained from specimens prepared by use of such techniques have revealed characteristic microstructural patterns of smectite clays as shown in Figs 5-7.

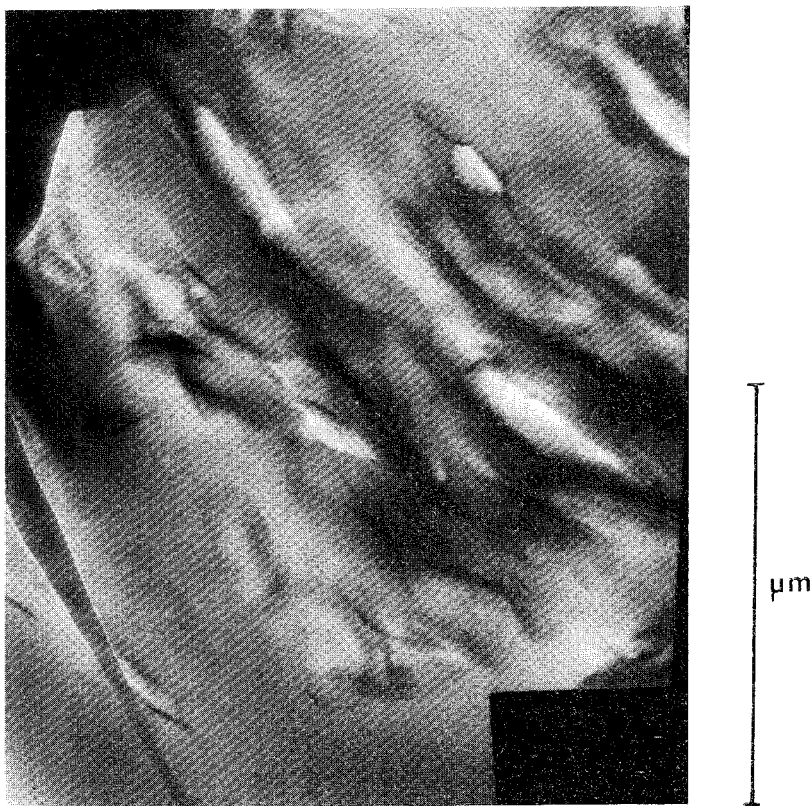


Fig 5. Electron micrograph of ultrathin section of butyl/methyl methacrylate-treated clay with a content of Na smectite (SWY-1) of about 100 %. Bulk density 1.25 g/cm³

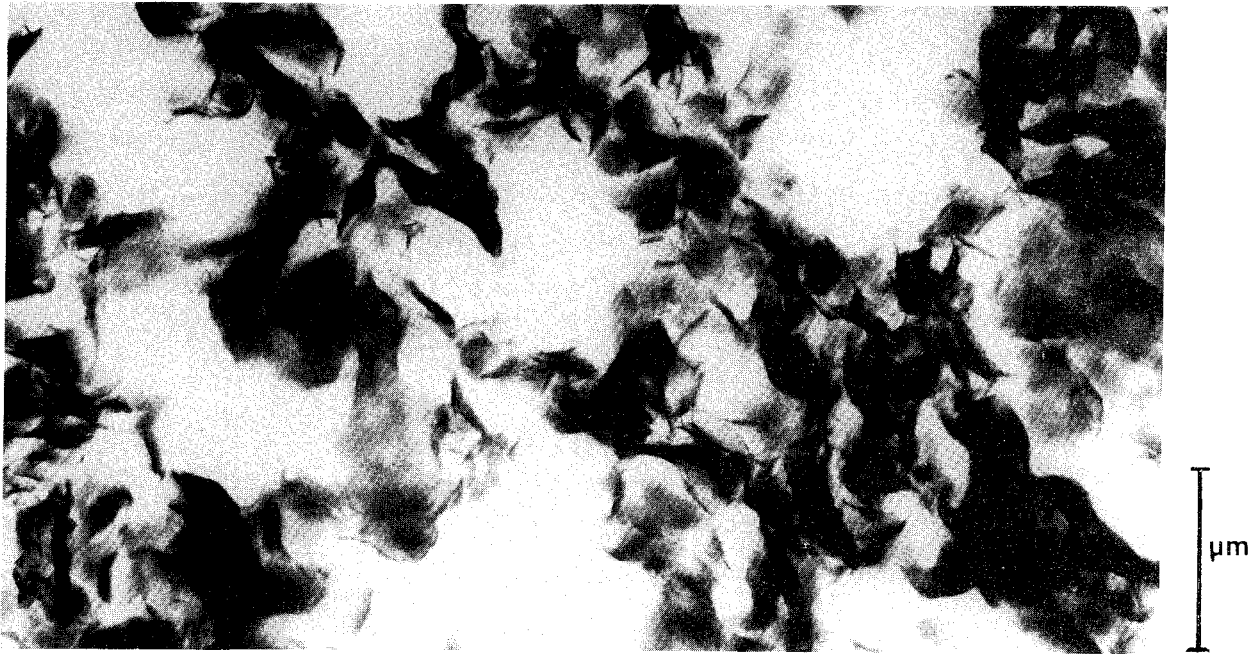


Fig 6. Electron micrograph of ultrathin section of butyl/methyl methacrylate-treated clay with a content of Na smectite (GEKO/OI bentonite) of about 70%. Bulk density about 1.6 g/cm^3

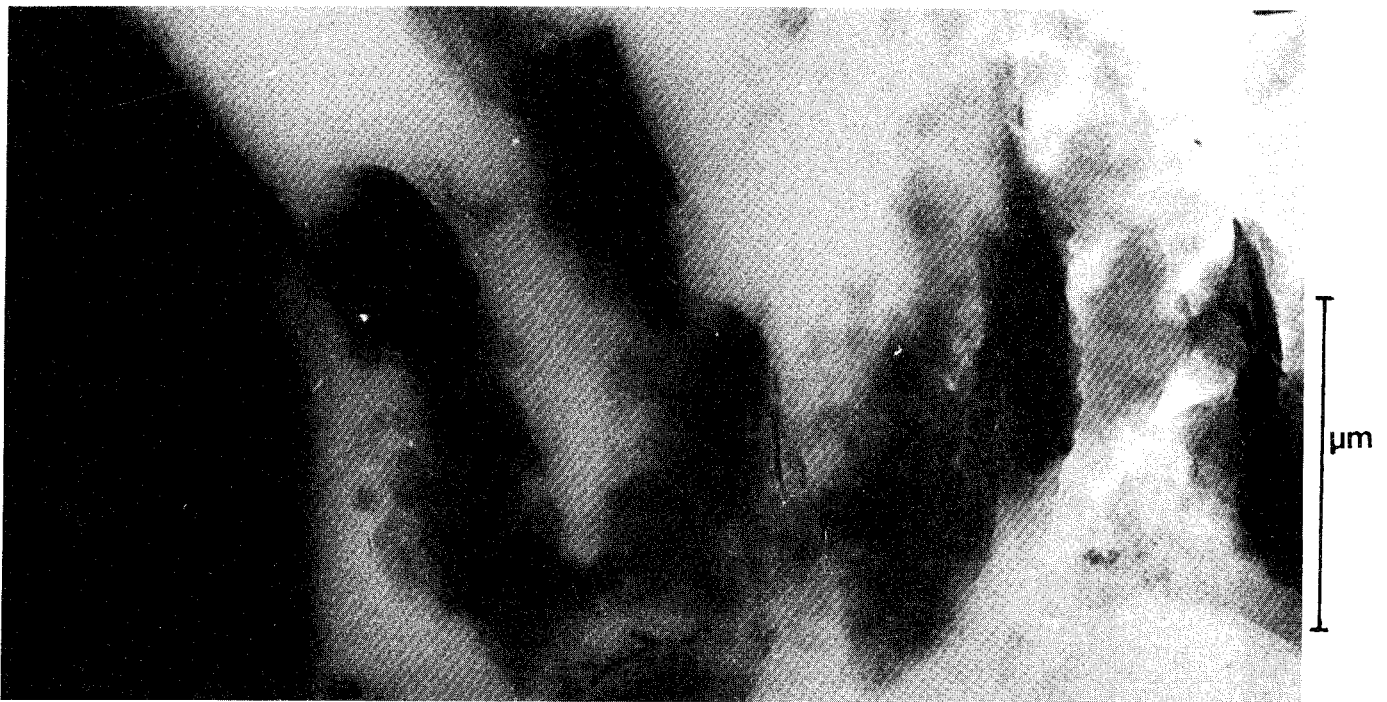


Fig 7. Electron micrograph of ultrathin section of butyl/methyl methacrylate-treated Triassic clay rich in Na montmorillonite. Bulk density about 2.3 t/m^3

2.3 Pore water, internal and external water

2.3.1 General

It is concluded from a number of published microstructural investigations that dense face-to-face grouping of smectite flakes is the dominant mode of association at high bulk densities. The water contained between closely located flakes is suitably termed interlamellar or internal water (6). At very low densities there seems to be evidence of edge-to-face coupling (7, 8, 9) although the exact nature of interparticle contacts has not been revealed. In principle, the particle arrangement may be of either type shown schematically in Fig 8, which illustrates the general appearance of smectite flake networks at low bulk densities. Case A, in which face-to-face association is the main structural fashion, may be more plausible than the edge-to-face type since it would explain why there is a significant potential for expansion even at bulk densities as low as 1.3-1.4 g/cm³ at Li or Na saturation. An additional reason for this is that the particle links, which may be more accurately described as tactoids, always seem to consist of several face-to-face grouped flakes. It cannot be excluded, however, that both versions apply, Case A resulting from expansion from denser states, while Case B may be valid for sediments formed by successive association of discrete particles.



Fig 8. Microstructure of smectite clays at low bulk densities

The matter of particle distribution is essential for the evaluation of the physical state of the pore water, one possible way of estimating the ratio of internal and external water being based on electron microscopy as demonstrated in the subsequent text.

2.3.2 Quantitative microstructural analysis

Detailed microstructural investigations are preferably made by applying a technique based on ultramicrotome sectioning and transmission electron microscopy. The preparation of undisturbed natural clay specimens usually involves stepwise replacement of the pore water with plastic monomer by diffusion. The monomer used in the author's study was butyl/methyl methacrylate with which the samples were saturated after having replaced the porewater with 99.5 % ethylene alcohole in successive steps (5). The 0.25 cm³ specimens were completely confined between porous filters in sample holders throughout the chemical treatment to prevent expansion. After polymerization at 60°C for one day, ultra-thin sections (300-500 Å) for electron microscopy were taken perpendicular to the plane of sedimentation or general stratification by means of an ultramicrotome equipped with a diamond knife.

The microstructural patterns as illustrated by electron micrographs can be analysed by simple statistical methods (11) provided that the ultrathin sections have a standard thickness (300-500 Å). The total sectioned pore area (P) in percent of the total area (T) of the micrograph and the pore size (a_p) are characteristic microstructural parameters. The pore size is defined as the longest intercept (Fig 9).

The measurement of pore size (individual measurements) and pore area (continuous line integration) was based on drawn images of the micrographs in which no discrete particles are depicted. Hence, the drawings show black areas for the clay particle matrix with no sectioned pore space. Depending on particle size and arrangement this matrix has a varying density which is not illustrated by the even black areas, which means that the true porosity cannot be judged from the drawings. Although the sections are extremely thin they naturally contain very small voids which are embedded in the clay sections and are thus not revealed. The observed frequency of pores containing external water and being smaller than about 1000 Å is therefore not representative and needs to be corrected.

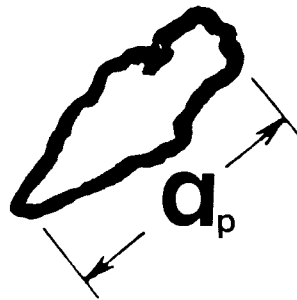
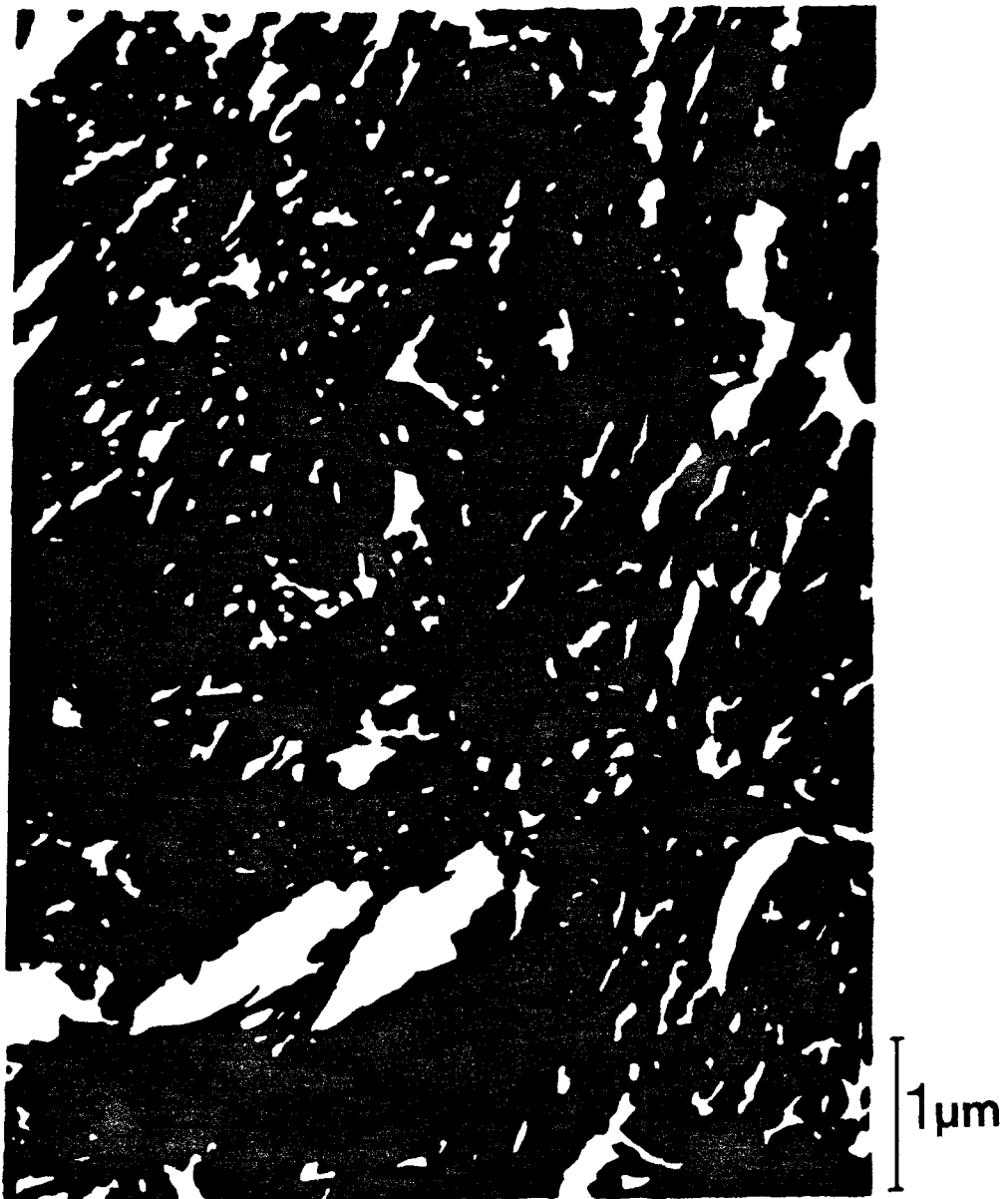


Fig 9. Example of schematic reproduction of electron micrographs. The continuous particle network is marked black without reference to variations in density. The pore system consisting of discrete, sectioned pores defined in the picture, is marked white

Statistical treatment of drawn images of natural clays with smectite as major mineral in the clay fraction has yielded the values in Table 1, each sample being represented by 5 micrographs as an average. The majority of the measurable pores in most of the investigated clays belonged to the "ultra-pore" fraction ($<0.2\mu\text{m}$). The largest average pore size was found for the relatively soft montmorillonitic Cretaceous Fish clay and the Tertiary clays, while the smallest average pore size was found for the montmorillonitic Ordovician and Triassic clays. The micrographs usually had a magnification of 10.000-25.000 X.

Table 1. Natural smectite clays analysed with respect to their microstructural features and physical properties (12)

Clay	Bulk dens g/cm ³	Water cont %	Poro- sity* %	Clay cont ($<2\mu\text{m}$) %	Clay minerals**	Microstruct param Median pore size μm	P/T %
Ordovician Kinnekulle bentonite	1.98	28	43	38	S>Ch1>K	0.12	1.5
Triassic Vallåkra clay	2.30	10	21	10	S>H>K>Ch1	0.12	7.0
Cretaceous "Fish" clay	1.88	34	47	43	S>K	0.30	12.7
Tertiary London clay	1.87	35	49	47	H>S>K>Ch1	0.29	14.5
Tertiary Røsnaes clay	1.83	38	51	65	S>H>K>Ch1	0.33	15.8

* Ratio of pore volume to total volume

** S=smectite and mixed layers, H=hydrous mica, Ch1=chlorite, K=kaolinite

The "microstructural porosity" P/T is a function of the pore size. Thus, the highest P/T-values were found for the clays with the largest average pore size. The reproducibility of the values of the structural parameters was very good and there was a clear tendency towards a certain pore size distribution and a certain P/T-range already when only one or two micrographs of each clay had been studied.

The P/T-values can be transformed to three-dimensional porosities from which the ratio of the volume of external water and that of total volume (V_e/V) can be evaluated. It is about 0.001 for the Ordovician clay, 0.02 for the Triassic clay, 0.05 for the Cretaceous clay and approximately 0.06 for the Tertiary clays. Using these figures and the actual porosities representing the space occupied by internal as well as external water and defined as $(V_i + V_e)/V$, the ratio V_i/V_e of internal and external water can be calculated. With the exception of the Ordovician clay we find the value to be surprisingly constant, i.e. ranging between about 7.5 and 9.5 for the investigated bulk density interval. All the clays have sodium as major adsorbed cation except the Fish clay, which is Ca-saturated. The Ordovician clay gave a much higher V_i/V_e -ratio which is probably explained by its very high Na smectite content and relatively high density.

Naturally, the evaluated amounts of internal water from the micrographs include some external water. Thus, the "opaque" particle aggregates contain intra-aggregate external water enclosed in voids with a maximum diameter of about 1000 Å. This amount is assumed to represent about 20-50 % of the volume of internal water evaluated from the microscopy, which brings down the actual V_i/V_e -ratio and in turn suggests that the "true" internal water constitutes about 70-85 % of the total water content of the investigated dense natural clays.

Recent studies of soft, artificially produced clay-water mixtures, illustrated here by Fig 6, have given similar results. Thus, sodium montmorillonite clay prepared by saturating air-dry, fine-grained clay powder with brackish water while confined in oedometers, yielded a clay with tactoid-type microstructure characterized by a median a -value of 0.25 μm and a P/T-value of 28 %, the bulk density being 1.6^p

t/m³. Applying the same philosophy as for the dense natural clays, the internal water is concluded to represent 40-60 % of the total water content of this soft clay.

An even softer sodium montmorillonite clay gel, produced in a similar way as the previous one but using distilled water, gave electron micrographs like the one shown in Fig 5. The bulk density was 1.25 t/m³ and the water content about 215 %. We see from this picture that the smectite flakes, most of which appear to have a length of more than 0.1-0.2 μm , are collected in packs of 5 - or more - aligned flakes in much the same way as Case A in Fig 8. The P/T-value of this clay is 31 %, which yields a V_i/V_e ratio of 0.35-1.2, meaning that the internal water represents 20-50 % of the total water content. The frequency of small voids in the clay matrix, holding external water, is much higher than in the denser smectite clays and the "true" internal water therefore represents a much smaller fraction. A plausible figure expressed in percent of the total porewater volume is 10-20.

2.3.3 Conclusions

The microstructural analysis demonstrates that the clay matrix of smectite-rich materials holds an amount of internal (interlamellar) water that is related to the external (pore) water in a fashion that is largely determined by the bulk density. The porewater chemistry should also be a determinant according to classical colloid chemistry in the sense that an increase in ion strength produces coagulation of particles. However, we will make the distinction here that interlamellar space hosts 3 hydrate layers at maximum. This criterion implies that anions are not present in the interlamellar space because of Donnan exclusion and that electrical double-layers are developed only in pores holding external water.

For any particular pore water salinity there is a unique relationship between internal and external water. The data derived in the preceding text suggest a general relationship of the type shown in Fig 10. We will see later that additional restrictions yield even lower percentages of internal water.

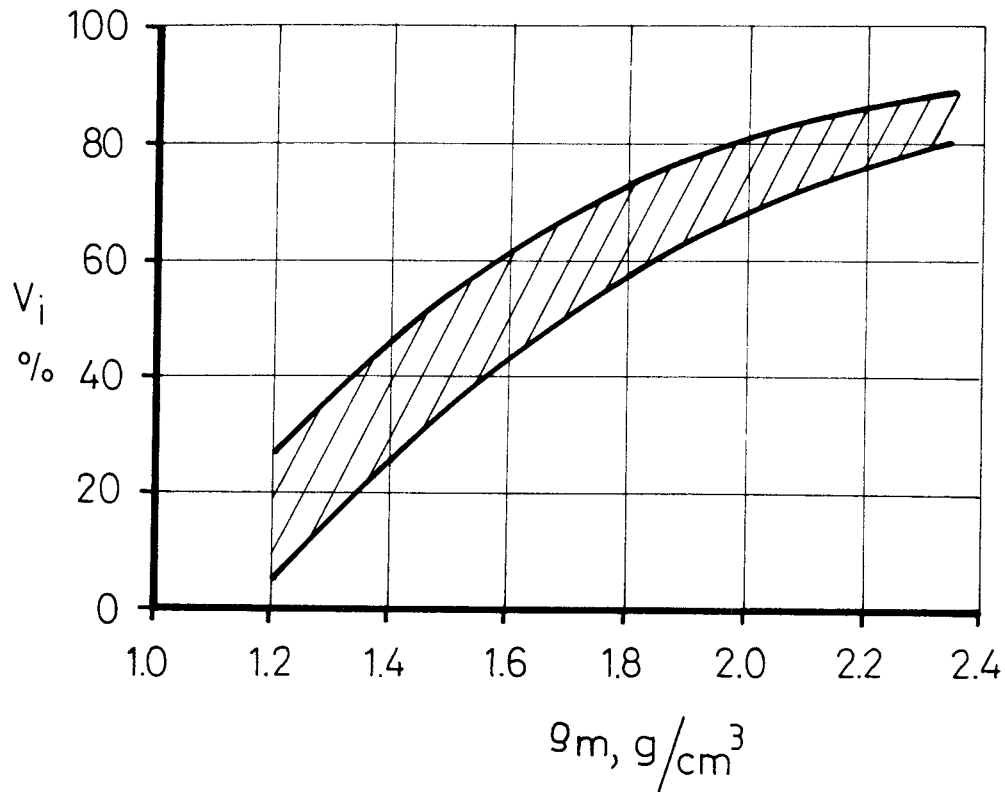


Fig 10. General relationship between bulk density and content of internal water in percent of the total pore water volume of smectite clays

3 CLAY-WATER INTERACTIONS

3.1 Current concepts of smectite-adsorbed water

3.1.1 Recent literature review

Sposito & Prost (13) recently synthesized available empirical information on the physical state of smectite-adsorbed water from which they drew conclusions as to the spatial organization of the adsorbed water molecules, the mechanism of hydration of smectites, and the thickness of the layer of adsorbed water whose molecular vibration properties are significantly affected by the clay mineral surfaces. Their main conclusions, which are taken here as the state of art, form the basis of this chapter.

- * The deficit of positive crystal lattice charge is of profound importance. If it occurs in the octahedral sheet the adsorbed water molecules should form only weak hydrogen bonds with the surface oxygen atoms, while strong hydrogen bonds are expected to be established near sites of isomorphous substitution in the tetrahedral sheets. For the EF model of montmorillonite, hydrogen bonding should be strong.
- * A general conclusion from various infrared spectroscopic studies of smectite hydration is that solvation of the exchangeable cations by either three (monovalent ions) or more (bivalent ions) water molecules forms the first stage of water adsorption. It leads to interlamellar spacings expanded to accommodate one or two layers of adsorbed water molecules. Additional hydration can be assumed to result in the formation of solvation complexes or sheaths for the exchangeable cations, which is the traditional view of smectite hydration.
- * Proton motion studies of Li montmorillonite using neutron scattering technique indicate that water molecules adsorbed to form 1-2 hydrate layers diffuse much more slowly than those in bulk water, and that they are not rigidly bound to the exchangeable cations. This suggests a considerable degree of freedom of adsorbed Li ions. Recent diffusion tests actually demonstrate that the same goes for Na (14).
- * Investigations of dielectric relaxation properties of montmorillonite saturated with monovalent, exchangeable cations, indicate that interlamellar monolayers consist of water molecules arranged in a strained, ice-like pattern with bonds formed with the oxygens of the silicate surface (Fig 11). At least some of the molecules in this monolayer are thought to be strongly associated with these oxygens in contrast to montmorillonite with Ca as exchangeable ion, in which case the cation tends to bind solvation shell water so strongly that the water lattice is disturbed.

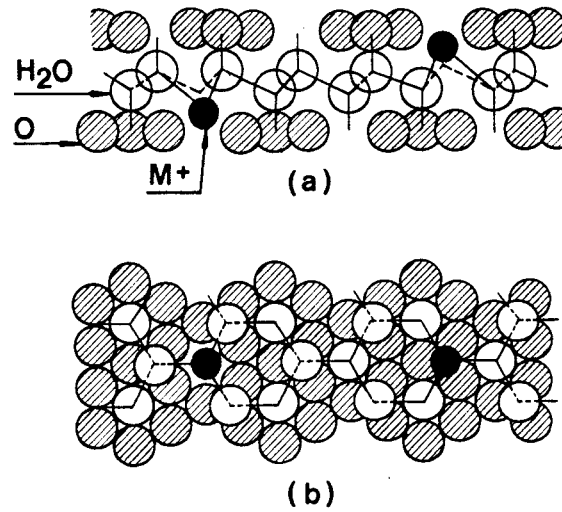


Fig 11. Spatial arrangement of water molecules in the interlamellar space of montmorillonite containing monovalent exchangeable cations, as determined by dielectric relaxation spectroscopy: (a) section view, (b) plan view. The shaded circles denote clay surface oxygen atoms (13)

- * Thermodynamic data cannot be interpreted directly in terms of molecular structure since any specific entropy or energy value is an average over the entire clay-water system (internal + external water) and cannot be attributed to part of the water alone. This point is of particular importance since it implies that parameter values from any measurement of the physical state of the porewater only mirrors some average conditions which cannot be used for derivation of the structure of interlamellar water. Thus, not only entropy and IR measurements but also NMR analysis of water saturated clays are disqualified if they are not interpreted with due respect to the relative amounts of internal and external water.
- * It is concluded from thermo-dilatometric measurements that the structure of water adsorbed by Na montmorillonite is more extensible and compressible but also less fractured than the structure of bulk liquid water

Synthesizing all this and referring to the two basic montmorillonite structures, the following extremes can be defined:

- 1 Hydration of the Edelman/Favejee structure takes place through formation of an ice-like hydrogen-bonded water lattice that grows from the protruding hydroxyls, forming a regular water lattice that matches that of the surface. It is required, however, that interlamellar cations are sized and charged so as not to disturb the water lattice. The necessary conclusion is that the molecules are not as closely packed as those in bulk water.

- 2 Wetting of the Hofmann/Endell/Wilm structure has the form of hydration of interlamellar cations through electrostatic bonds. Like in the case of the EF model, interlamellar water lattices may be established but the spatial arrangement of the water molecules is largely determined by the position, size and charge of interlamellar exchangeable cations, which in turn depend on the location of the deficit of positive clay lattice charge. The orientation and mutual interaction of the water molecules as well as their association with the interlamellar cations and the crystal lattice become altered in the successive build-up of interlamellar hydrates, the expected degree of ordering being low, particularly of the second and third hydrates. The molecular arrangement may thus vary and yield a density that is higher than, equal to, or lower than that of free water. Close packing would result from complete absence of hydrogen bonds and an appropriate concentration and charge of interlamellar cations, while an open arrangement may result from hydrogen bonds formed between the oxygen atoms of the basal planes and neighboring water molecules.

It is highly probable that various intermediate stages exist between these extremes, but it appears to be virtually impossible to identify or even characterize them. What we intend to do here is to find out what the density is of the interlamellar water under circumstances that should reveal whether the EF-version is valid at all, and if the EF-related hydration model outlined in the preceding paragraph 1 is relevant. For this purpose we will examine Forslind's hydration

theory in the first place, some recent thermodynamic considerations, and some precision dilatometer tests thereafter. As will be shown, all three approaches are rather clarifying with respect to the validity of Forslind's model although the matter cannot be considered as settled.

3.1.2 The Forslind concept

Forslind introduced a structural model for interlamellar water that is based on the Edelman/Favejee crystal version. Objections were originally raised against the EF model since it yields a six times higher cation exchange capacity than the usually found experimental value if the apices carrying acidic hydroxyl groups are assumed to exchange their protons. This is because there are four unit charges per unit cell, while the average value observed is two-thirds of a charge unit per cell. This discrepancy has been explained by considering the coupling between the associated water lattice, which can be assumed to be of the ice-lattice type, and the basal planes of the montmorillonite crystallites. Fig 12 shows the protruding hydroxyls of the (001) plane with three unit cells marked, while Fig 13 shows the basal molecules of an ice lattice superimposed on these hydroxyls. It is immediately seen that there are only four hydrogen bonds formed between the three unit cells and the associated water lattice and the charge of the crystallite should therefore attain a mean value of two-thirds of a charge unit per unit crystal cell.

There are two particularly strong facts which are in favor with this model. Firstly, the phenomenon that hydrophilic clays always become negatively charged in aqueous solutions may generally be explained by proton expulsion, independently of whether there are isomorphous substitutions and lattice vacancies or not. Secondly, chemical studies of the interaction of Na-montmorillonite and glass with aqueous media have demonstrated that Si(OH)_4 is an important constituent of montmorillonite and that the pH of the medium is a sensitive function of its ionic strength (16). Thus, the pH-producing property of the Si(OH)_4 is clearly associated with the surface constitution of montmorillonite and this may be fully explained by the reactivity of the surface hydroxyls of the EF crystal model.

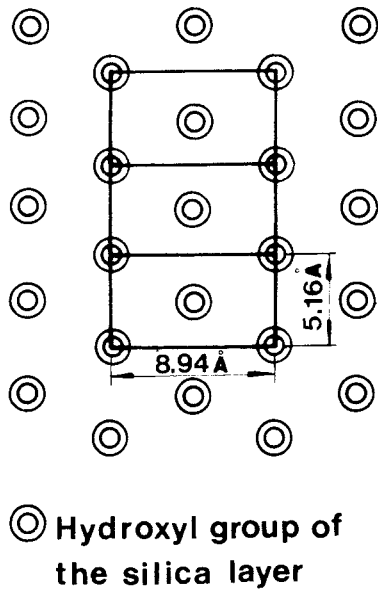


Fig 12. Plan view of the (001) plane of the EF crystal model

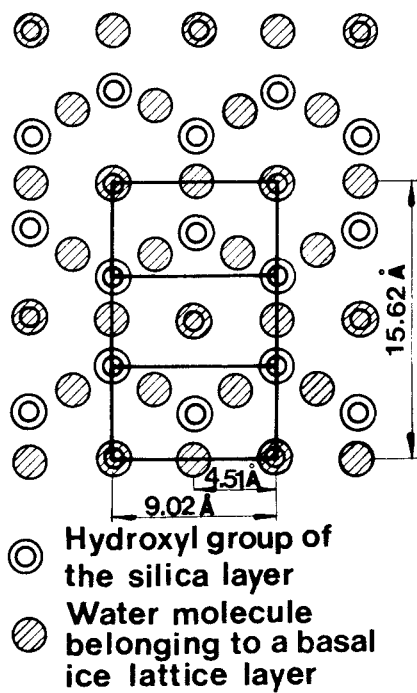


Fig 13. Basal ice lattice layer superimposed on the crystal plane in Fig 12. (After Forslind)

Forslind stated that thermal alteration of montmorillonite in the form of endothermal lattice reorganization indicated by use of DTA around 100°C is associated with surface phenomena. He ascribed such surface reorganization to a reequilibration of the SiO_2 lattice, disturbed by surface dehydroxylation. The structural effect of heating to about 100°C would be that of trans-cis conversion of the silica layers, or in practice, a transformation from the EF to the HEW state. Thus, experimentally observed basal spacings and theoretically deduced charge distributions are in reasonable accordance with the EF model as illustrated by the commonly measured basal spacing of 12.4 Å of air-dry montmorillonite which corresponds to the spacing of directly interacting protruding hydroxyls, slightly expanded in the c-axis direction due to intercalated interstitial ions (cf Fig 14). At 12.4 Å spacing, 23 % of the protruding hydroxyls remain intact while 77 % are replaced by water molecules to fill the matrix, and together they contribute 39 electrons to the intercrystalline space. Adding to this the contribution from the interstitial molecules, i.e. 20 electrons, the total number of electrons in the intercrystalline layer is 59 electrons per unit cell which is in satisfactory agreement with observations. Forslind concluded on this basis that the EF structure is in agreement with experimental data and that it fits montmorillonite Fourier syntheses while the HEW model does not.

When hydration takes place an unstable state with a basal spacing of 15.05 Å is first reached according to the model (Fig 14). It is followed by the establishment of one complete water layer with a lattice of the type shown in the diagram between adjacent clay crystal surfaces. The average number of water molecules per cell is 5.33 (16 molecules per three cells) or 0.119 g H_2O /g clay, corresponding to a theoretical basal spacing of 17.81 Å. The density of the water is significantly less than unity and its attachment to the mineral substrate is supposed to provide a strong but very flexible medium joining the two crystallites.

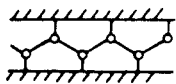
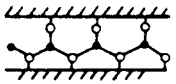
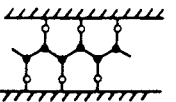
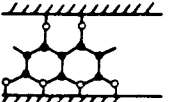
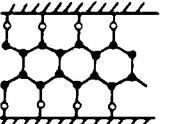
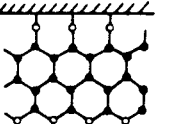
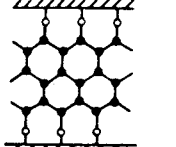
Further increase in water content yields an unstable state with a basal spacing of 18.73 Å, which is transferred to a stable state with two hydrates, a basal spacing of 21.49 Å and a water content of 0.238 g H_2O /g clay if expansion is allowed for. A third stable state

with a basal spacing of 25.17 Å is obtained on additional wetting according to Forslind.

The density of the interlamellar water is actually a matter of definition. Considering only the water molecules grouped between the apical hydroxyls we find that one stable monolayer of water molecules, as derived from atomic mass data, would be about 0.5 g/cm³, while that of two and three hydrates would be approximately 0.6 and 0.7 g/cm³, respectively.

3.1.3 Energy considerations

Many attempts have been made to evaluate the energy state of water absorbed by montmorillonite but only recently, sufficiently careful and relevant measurements and evaluations have been made that offer reasonably safe conclusions. These studies comprise an appropriate distinction between internal and external water and are therefore of interest in the present context (18). Wyoming montmorillonite, saturated with Li, Na, Ca, Zn, Cd and Cu, a Li-hectorite and an endellite clay were used because of their different pore systems, the testing being made by applying RMN and IR techniques at different degrees of hydration. The investigators concluded that the water in larger pores, i.e. the external water, resembles free water while interlamellar water has an energy state that is similar to that of ice. They stated, on the basis of their tests, that the hydration energy is much higher of Mg²⁺, Ca²⁺, Sr²⁺ and Ba²⁺ than of Li⁺, Na⁺, Cs⁺ and K⁺. In principle, therefore, their findings are not incompatible with Forslind's model of interlamellar water that is directly associated with the crystal lattice in the particular case of Li or Na as adsorbed cations.

Schematic interlayer structure	H ₂ O molecules per unit cell	Basal spacing, Å	g H ₂ O/g clay	mM H ₂ O/g clay	Remarks
	0	12.30	0; 0,084 ^a	0; 4.667 ^a	Unstable; no hydration; four OH groups per unit cell
	2.66	15.05	0.059	3.278	Unstable
	5.33	17.81	0.119	6.661	Stable monolayer
	8.0	18.73	0.179	9.944	Unstable
	10.67	21.49	0.238	13.222	Stable; two layers
	13.32	22.41	0.297	16.5	Unstable
	16.0	25.17	0.357	19.833	Stable; three layers

^a At complete dehydroxylation.

Fig 14. Water lattice configuration in interlamellar positions of Li- or Na montmorillonite (After Forslind)

3.1.4 The porewater density

Several attempts have been made to determine the porewater density, most of the reported values being in the range of 0.85-1.4 t/m³. One of the most careful studies was made by Low & Anderson, deserving special attention since it covered a relatively wide bulk density range and several electrolytes, and since the experimental error was as low as ± 0.0029 g/cm³ (19). They investigated water saturated montmorillonite clay refined from Wyoming bentonite and applied a form of dilatometry in a series of tests of Li, Na and K-saturated clay. After degassing the clay with a Hi-vac pump at 105°C it was saturated with freshly-boiled deionized water for about 8 hours. The paste was then compressed between a porous filter and a column of mercury and, by means of capillaries, the change in volume of the paste and the volume of water forced through the filter was measured simultaneously. Fig 15 show data calculated from Li and Na montmorillonite experiments, using the term \bar{v}_w for the partial specific volume and assuming complete dispersion and parallel orientation of all mineral flakes. They did not consider the existence of external water, which must have amounted to at least about 30 % of the total porewater content at the highest density, and to more than 95 % at the lowest density. Nor did they consider the compressibility of the porewater, but this omission does not significantly affect the evaluated densities.

These investigators expressed the change in specific volume in terms of a successive drop in porewater density at decreasing distance from the basal planes of the crystals and found that the average porewater density at average water contents of 50-100 % was 0.97-0.98 g/cm³ at room temperature (Fig 16). For the sodium- and lithium-saturated samples the density values tended to be lower than for the potassium-saturated clay indicating a lattice-disturbing property of the K ion, which is significantly bigger than the other investigated cations.

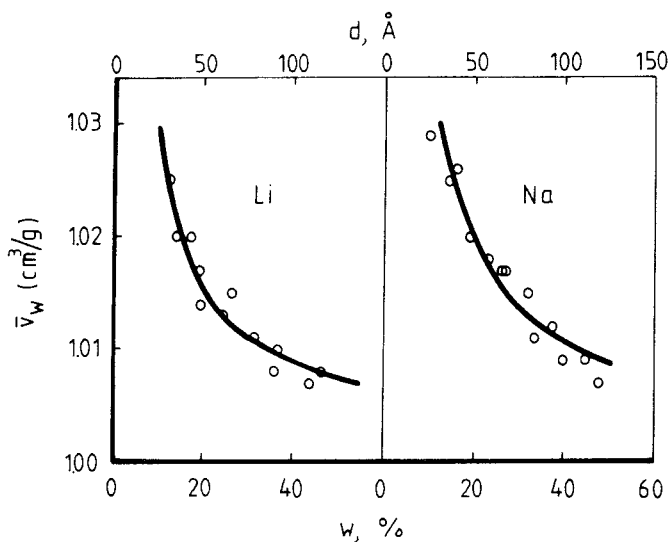


Fig 15. The partial specific volume of the porewater at room temperature (25°C) as a function of the average water content (21).
 w = water content, d = interlayer distance

Their conclusions were that the ordering of the water was altered to a distance of at least 60 Å from the basal planes. We will consider these values in detail later but at this stage already, we like to point out the interesting fact that if the density 0.993 g/cm³ for 480 % water content of Na montmorillonite is reinterpreted to yield a density of 1.00 g/cm³ for the external water, which can be assumed to have formed at least 97 % of the total water content, and a separate density of the remaining interlamellar water, the latter is found to be 0.77 g/cm³. Repeating the calculation for 80 % total water content, which corresponds to a bulk density of 1.54 t/m³ and an estimated fraction of external water of 70 %, we find the density of the interlamellar water to be 0.91 g/cm³. Extrapolating the curve to 50 % water content, i.e. a bulk density of 1.72 g/cm³ with an estimated percentage of external porewater of 60, the calculated density of the interlamellar water constituting the remaining 40 %, is 0.93 g/cm³. These estimations indicate that the interlamellar water may have a significantly lower density than free pore water if Low & Anderson's

values are correct and if we consider the fact that the interlamellar water only forms a fraction of the total water content and furthermore assume that only interlamellar water can be organized to form open lattices.

From a separate series of tests, in which the volume changes of a very soft Na montmorillonite clay gel were measured before and after mechanical agitation, the investigators concluded that the changes were unexpectedly small (20). Actually, they were less than 1 % of the predicted value, which was taken to indicate that the water structure nearest the clay particles was left relatively undisturbed. An alternative explanation, that is favored by the present authors, is that the amount of interlamellar water was insignificant in the clay gel that appears to have had a density of somewhat less than 1.1 t/m³.

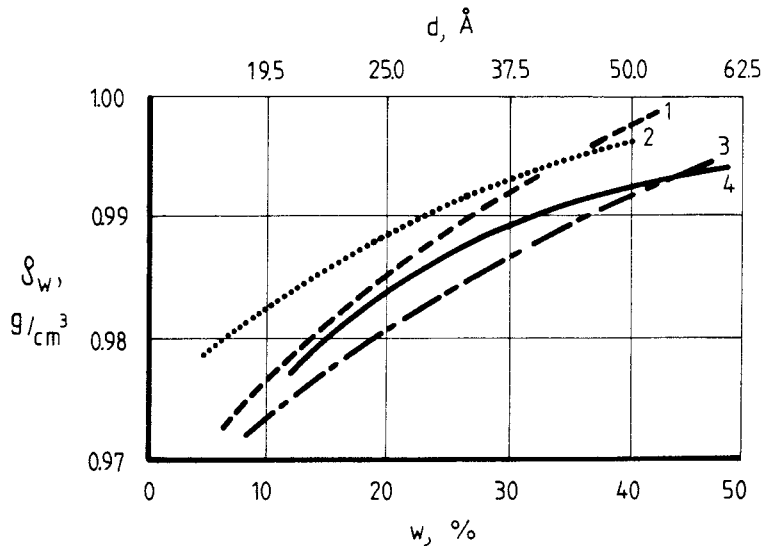


Fig 16. The average density (ρ_w) of porewater in montmorillonite as a function of water content (w) and electrolyte according to Low & Anderson. 1) K-clay at 1°C, 2) K-clay at 25°C, 3) Na-clay at 25°C, 4) Li-clay at 25°C

3.2 Conclusions

The major issue that we are concerned with, i.e. the physical state of the internal water, appears to be closely related to the question concerning what crystal lattice model that is actually valid. While X-ray diffraction analysis and chemical analyses do not offer means of distinguishing between the HEW and EF structures, it follows from the preceding text that careful determination of the density of interlamellar water opens up a line of approach. However, a different technique than that of Low & Anderson would be preferable in order to avoid repeating possible experimental errors. As pointed out, it is essential to consider the spatial arrangement of the montmorillonite flakes since it determines the relative amount of internal and external water. A more detailed picture of the microstructural features of montmorillonite clays of low and high density would be required to check the relationship given in Fig 10. It was therefore decided to conduct an exploratory study of the density of interlamellar water in montmorillonite clay, and to investigate its microstructural features by using new techniques.

4 EXPERIMENTAL

4.1 Test philosophy

The dilatometric technique used by Low & Anderson and others involved compression of a soft clay gel with simultaneous careful measurement of the volume of the expelled water. For the present study an independent technique was asked for and the following measuring principle was found to be superior to other alternatives. It is based on the principle of saturating a montmorillonite paste of high bulk density and then introducing it into a water-filled closed vessel equipped a capillary for measuring the associated change in water volume. The dense sample is supposed to host a major part of the water in interlamellar positions, and introducing it in a large volume of free water may initially lead to further interlamellar hydration and subsequently to particle dispersion and an altered ratio of internal/external water. In the theoretical case of complete dispersion, the amount of internal water would vanish completely, which should be manifested by a downward motion of the capillary meniscus if the density of this water is lower than that of free water.

This measuring principle is estimated to yield average porewater densities with an accuracy of 0.001 g/cm^3 or better, provided that the following criteria are applied:

- 1 The water saturation of the dense clay paste must be complete before submerging it in the water of the vessel. At moderately high densities 100 % saturation is obtained by use of de-aired water that is introduced through a filter at one end of the dry sample, which is kept under vacuum at its other end. Through this procedure the amount of gas in the sample will be negligible.
- 2 A filter saturated with de-aired water should separate the vessel and the capillary so that the expansion of the clay does not extend into the capillary.
- 3 The temperature is controlled so that heat-induced volume changes are either eliminated or calculable.

The evaluation of the density of internal water requires a much improved understanding of the degree of dispersion and this matter was focussed on in a first phase of the study. The intention was to get a more detailed picture of the ordering of the montmorillonite flakes and, through this, a way of checking the relationship between the fractions of internal and external water that is implied by the diagram in Fig 10. A true vision would require Ultra-Microscopy or High Voltage Electron Microscopy of wet clay, the latter technique being available for the present study.

4.2 The hydration process in Na montmorillonite and the associated microstructural evolution

4.2.1 HVEM-microscopy

The detailed hydration of an initially dry montmorillonite clay was studied directly in the 3 MV microscope at the CNRS research centre in Toulouse, France. It was kindly put at the authors' disposal for a pilot study in which air-dry purified montmorillonite powder (SWY 1, Na Wyoming type) was placed in a cell that could be inserted in the electron path of the high voltage microscope. The cell was attached to a closed system for flushing water vapor of a given pressure through it, by which the original vacuum conditions were replaced in steps to reach the condition of 10 mm Hg to 60 mm Hg vapor pressure at room temperature. 10 mm Hg vapor pressure yields an RH value approximately equal to 50 % at room temperature, which corresponds to a water content of the clay of approximately 10-20 %, and to at least one monomolecular interlamellar hydrate. 20 mm Hg vapor pressure corresponds to RH=100 % and presumably 2 interlamellar hydrates, while 40 and 60 mm Hg would offer sufficiently much water to establish 3 hydrate layers of the unconfined clay and to fill small pores separating expanded stacks of montmorillonite flakes (cf. 22).

The outcome of the study, which comprised cyclic wetting and drying of the clay, has been discussed in a preliminary report (23). It demonstrated that the expected hydration and intra-aggregate swelling took place successively on wetting, as illustrated here by Fig 15 and 16. The gel is estimated to have reached a largely saturated state with an average bulk density on the order of 1.05 g/cm³ at the

highest vapor pressure, the depicted denser parts having a presumed density of about 1.3 g/cm^3 . An important fact is that the gel had become largely homogeneous in the last, fully expanded state, containing only a very small number of dense stacks and with most of the flakes rearranged into a very open honeycomb-type pattern. In this state, the amount of water in interlamellar positions is estimated to be less than 5 % of the total water content, while the corresponding percentage for the denser elements in the first wetting stage may have been as high as 60-80. These elements are estimated to represent a bulk density of about 2 g/cm^3 in a fully water saturated state. The study thus supports the general principle of distribution of internal and external water implied by the diagram in Fig 10 although the indicated content of internal water at low bulk densities appear to be somewhat too high.

It should be added here that the present study supports the conclusion from various electron microscopical investigations that single flakes do hardly exist. There is always a grouping of several flakes even when montmorillonite gels are free to expand, with the possible exception of Li-saturated clay (24, 25). The number of flakes that stick together in very diluted Na montmorillonite gels with porewater of low ionic strength appears to be very small, however, the maximum number being 5-10. The matter was further investigated in a later phase in conjunction with electron diffraction analyses of hydrating montmorillonite.

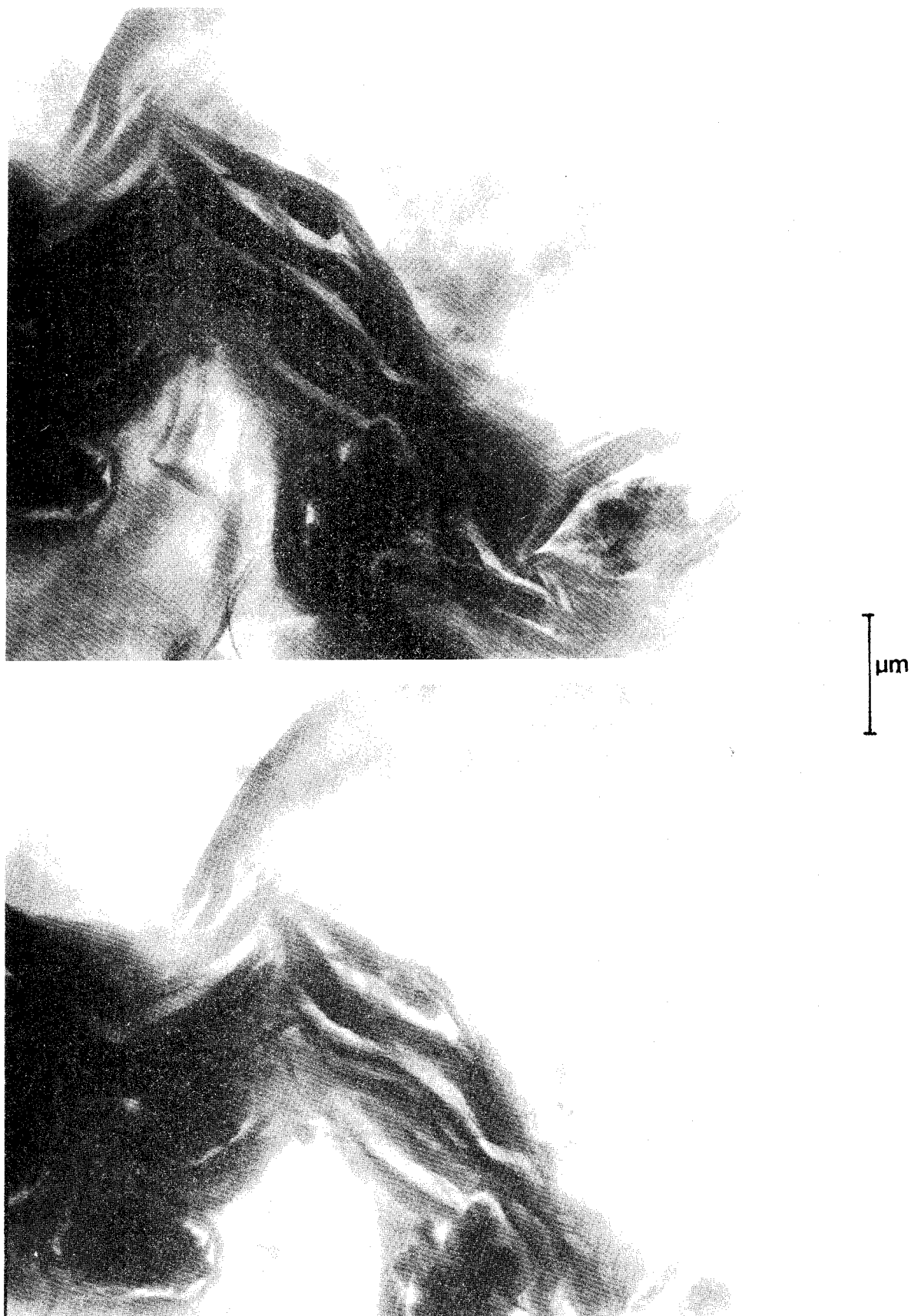


Fig 17. HVEM micrographs of hydrating montmorillonite clay. Upper: Initial condition of condensed large stacks. Lower: First wetting stage at 10 mm Hg vapor pressure, picture taken after 6 minutes

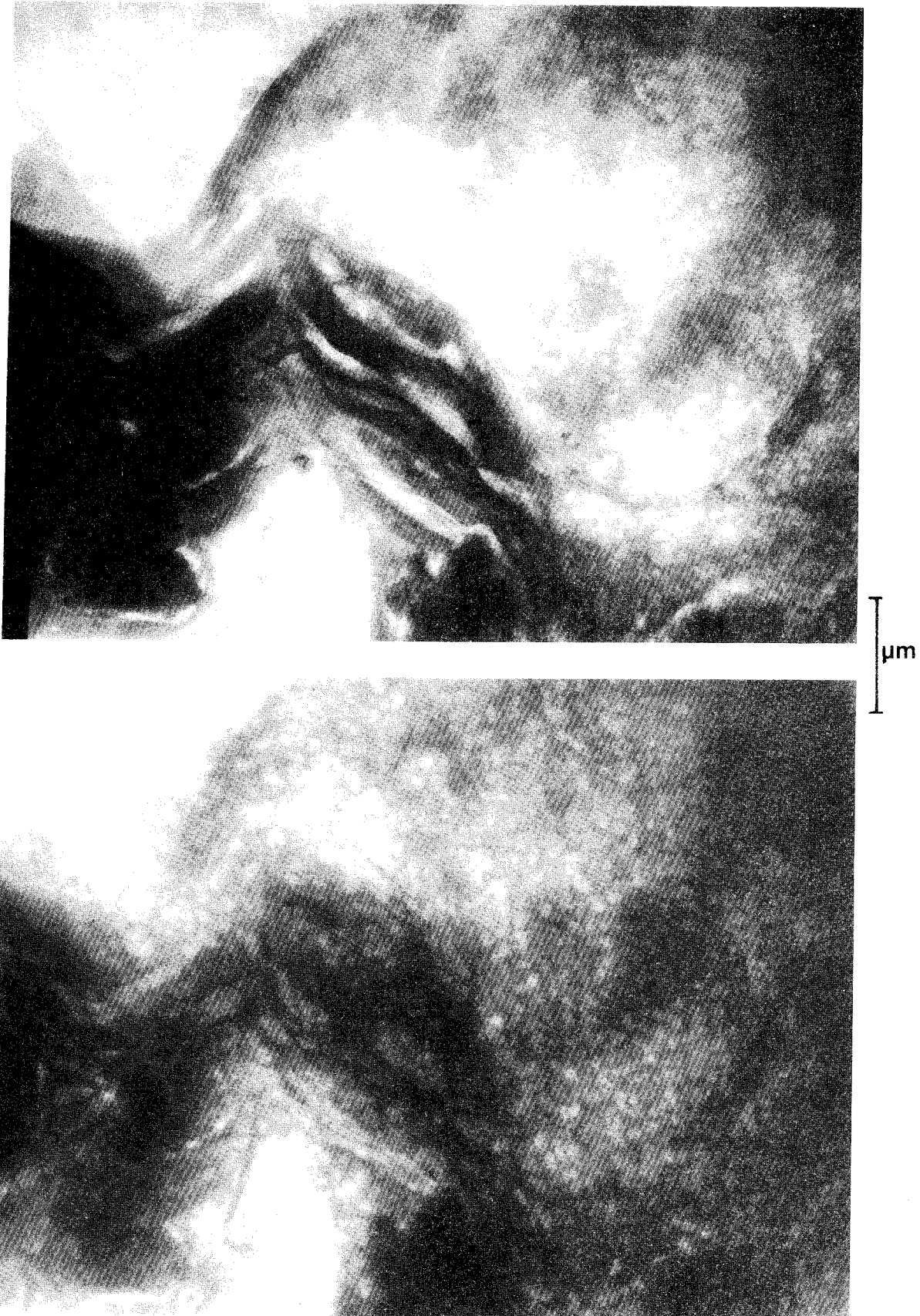


Fig 18. HVEM micrographs of hydrating montmorillonite clay. Upper: Second wetting stage at 20 mm Hg vapor pressure, picture taken after 1 minute. Lower: Third wetting stage at 40 mm Hg vapor pressure, depicting the ultimate state

4.2.2 Electron diffractometry

4.2.2.1 Orientation of crystal flakes in stacks

One of the major points in estimating how much of the total water in montmorillonite clay that is in interlamellar positions, is how regularly the individual crystal flakes are arranged, not only with respect to the parallelity of the basal planes but also to the orientation of their crystallographic a and b axes. Thus, it is obvious from various investigations that rotational distortion of several degrees of stacked flakes is common (2, 23).

The fact that selected area diffraction patterns of thin aggregates often show almost continuous rings or arced patterns demonstrates that the crystal axes a and b of many of the crystal sheets do not coincide. This suggests that the number of flakes in stacks with perfectly coinciding crystal axes does not exceed 5-10, which has a great impact on the evaluation of the amount of interlamellar water. Thus, it can be assumed that less than 90 % and probably only 60-80 % of the interlamellar space offers a possibility for regular water lattices to be formed. Using the diagram in Fig 10 it would mean that, for pure montmorillonite, the amount of internal water expressed in percent of the total porewater volume is probably less than 5% at a bulk density of 1.1-1.3 g/cm³, 40-60 % at a density of about 1.8 g/cm³, and 50-70 % at 2 g/cm³.

4.2.2.2 Electron diffraction of hydrating montmorillonite

Diffraction analysis of montmorillonite stacks with the direction of travel of the electron beam being perpendicular to the crystallographic a/b plane show clear ring-shaped patterns in vacuum. At hydration, these patterns are expected to become very diffuse and to disappear when the stacks become fully hydrated if the water molecules are randomly ordered, while the reflections are assumed to be only slightly distorted and even enhanced if the interlamellar water is organized to form quasicrystals of hydrated and expanded montmorillonite sheets. This issue was investigated in connection with the previously discussed HVEM study, the result of the diffraction study being illustrated by Fig 19. The micrograph at the upper left shows

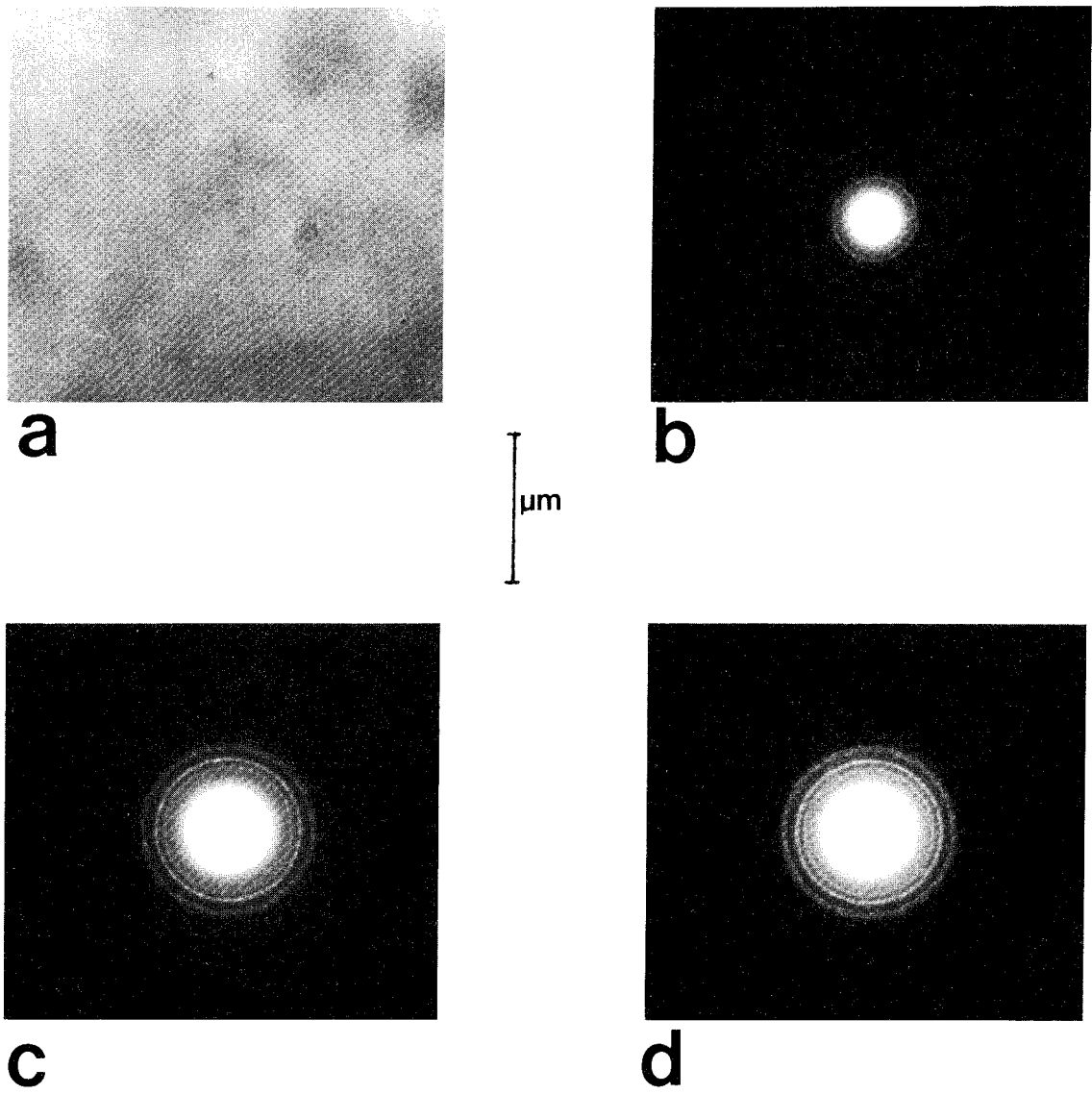


Fig 19. Electron diffraction patterns of a stack of montmorillonite flakes a) TEM picture, b) vacuum, c) 10 mm Hg vapor pressure, d) 20 mm Hg vp

the typical contour-less TEM appearance of thin stacks of montmorillonite flakes viewed approximately in the direction of the crystallographic c-axis. The micrograph at the upper right verifies that the stack consists of rotated flakes giving a vague pattern only. On hydration in 10 mm Hg vapor atmosphere, which corresponds to 1 monomolecular interlamellar hydrate, we see that the diffraction rings have become slightly more diffuse but also much more brilliant, while further hydration leading to two interlamellar hydrates yielded further enhanced diffraction rings. This supports the idea of rather well ordered interlamellar water. The voltage 2 MV, as well as the current and other settings that determined the intensity and focusing of the electron beam, were kept constant throughout the study.

4.3 Dilatometer tests

4.3.1 Test technique

4.3.1.1 **Pilot tests**

In a series of pilot tests clay gels with a bulk density of 1.04 g/cm³ were filled in pycnometers which were exposed to ultrasonic treatment. This was assumed to generate breakdown of possibly existing organized water lattices in the undisturbed clay and if its density had been lower than unity, as indicated by the determinations made by Low & Anderson, a decrease in volume and increase in density was expected to occur on disturbance, while a volume increase would logically take place after the end of the ultrasonic treatment. In the experiments this treatment was found to produce significant heat, for which due correction had to be made. The evaluation of the tests gave the same results as those of Low & Anderson, i.e. the average density of the porewater was insignificantly lower than unity. Since higher bulk densities could not be used in test setups of this sort, due to swelling pressures and insufficient disturbing power of the ultrasonic treatment, a different technique was applied in the main tests.

4.3.1.2 Main tests

A fully water saturated, dense sample of a clay rich in Na montmorillonite was inserted in a water-filled pycnometer to which a capillary was attached. The motion of the meniscus in the capillary as well as the temperature were measured as a function of time. The dense clay sample expanded to form a virtually homogeneous clay gel in the pycnometer.

The recorded change in volume of the clay/water system in the pycnometer as interpreted from the displacement of the meniscus in the calibrated capillary, was caused by the difference in density between the external and internal water, the amount of the latter being successively reduced in the course of the expansion.

4.3.2 Clay material

Commercial Na bentonite (MX-80) produced by the American Colloid Co was chosen for the study. Its clay content, i.e. the content of particles with a Stoke diameter less than 2 μm , is 80-90 % and this fraction has a montmorillonite content of 80-90 %. Fig 20 shows a typical X-ray diffractogram with a (001) peak displacement from 12.9 \AA to 17.4 \AA upon ethylene glycol treatment. Silt is the dominant remaining fraction which mainly contains quartz and feldspars as well as some micas, sulphides and oxides. The chemical composition is given by Table 2.

Spectrometric analyses have shown that the natural porewater of this clay contains 70 mg Na, 30 mg Ca and 15 mg Mg per liter porewater. This demonstrates that a significant amount of bivalent cations may be in interlamellar positions, but we assume here that this deviation from pure conditions is covered by the basic relationship between the assumed amounts of internal and external water.

Table 2. Representative chemical analysis of MX-80 bentonite (Asea-Atom)

SiO ₂	63.0 %
Al ₂ O ₃	16.1 %
Fe ₂ O ₃	3.0 %
CaO	1.1 %
MgO	1.6 %
Na ₂ O	2.2 %
K ₂ O	0.48 %
Li ₂ O	<0.01 %
MnO	0.03 %
TiO ₂	0.10 %
F	0.10 %
Cl	<0.01 %
S	0.12-0.23 %
Cu	<0.01 %
Zn	0.01 %
Cr	<0.01 %
Ni	<0.01 %
AsO ₄	0.018 %
NO ₃	none
PO ₄	0.060 %
S in sulphides	0.12 %

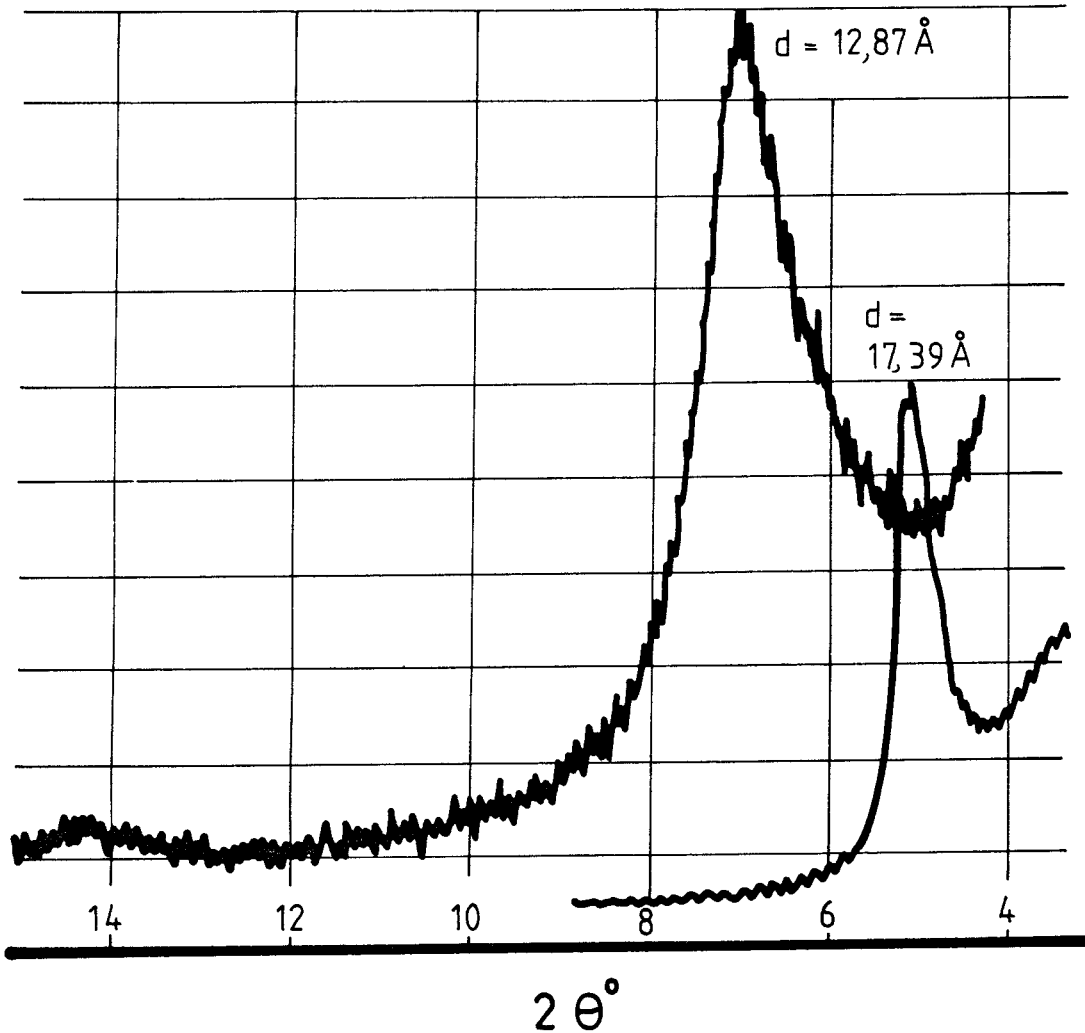


Fig 20. X-ray diffractogram of MX-80 powder. $2\theta^\circ$ is given by the horizontal scale. 12.87 Å is the 001 spacing of air-dry clay which is expanded to 17.39 Å by ethylene glycol treatment (lower curve)

4.3.3 Preparation of clay samples

Air-dry clay powder was compacted in a swelling pressure oedometer to a density that would yield a bulk density in the range of 1.80 to 2.20 g/cm³ at complete saturation (Fig 21).

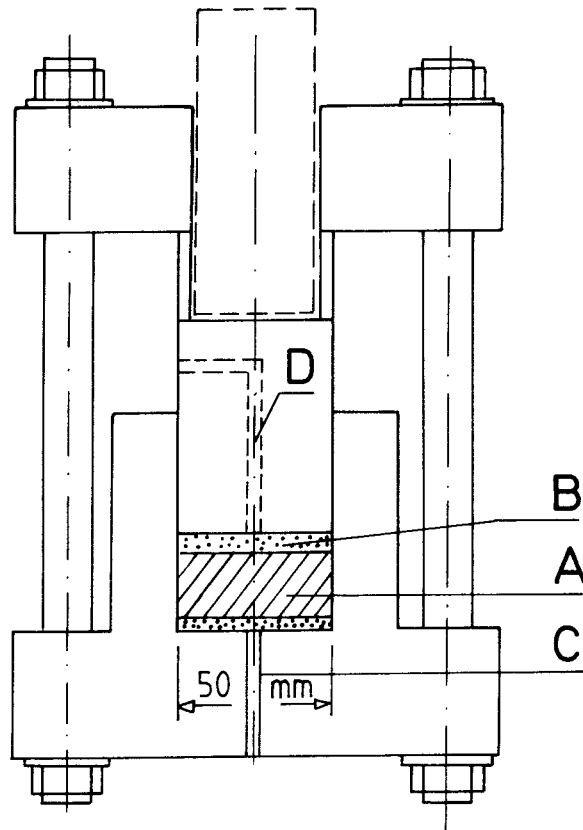


Fig 21. Swelling pressure oedometer used for preparation of saturated clay samples of high density. A) sample, B) stainless steel filter, C) water inlet, D) degassed passage

Distilled water was let in through the lower filter and successively filled the pores in the clay by which slight dissociation of exchangeable cations must have taken place. As indicated by electrophoretic tests the percentage of cations that were released cannot have exceeded about one percent, thus leaving the large majority of sodium ions in exchange positions.

The water uptake by the approximately 2 cm thick samples, which had a diameter of 5 cm, was known to be completed in less than a week as documented by a large number of similar tests, but they were kept in the oedometer for at least 10 days to assure that the degree of saturation had reached 100 %.

4.3.4 The pycnometer device

The 60 ml pycnometer was equipped with a glass filter that separated the interior from the capillary (Fig 22). After inserting the sample

of dense clay in the pycnometer, which was placed in a water bath, the motion of the meniscus in the capillary was recorded. The temperature of the bath was measured with an accuracy of $\pm 0.1^\circ\text{C}$ and due correction of the readings was made for the change in volume of the pycnometer, water content, and mineral substance that was caused by variations in temperature.

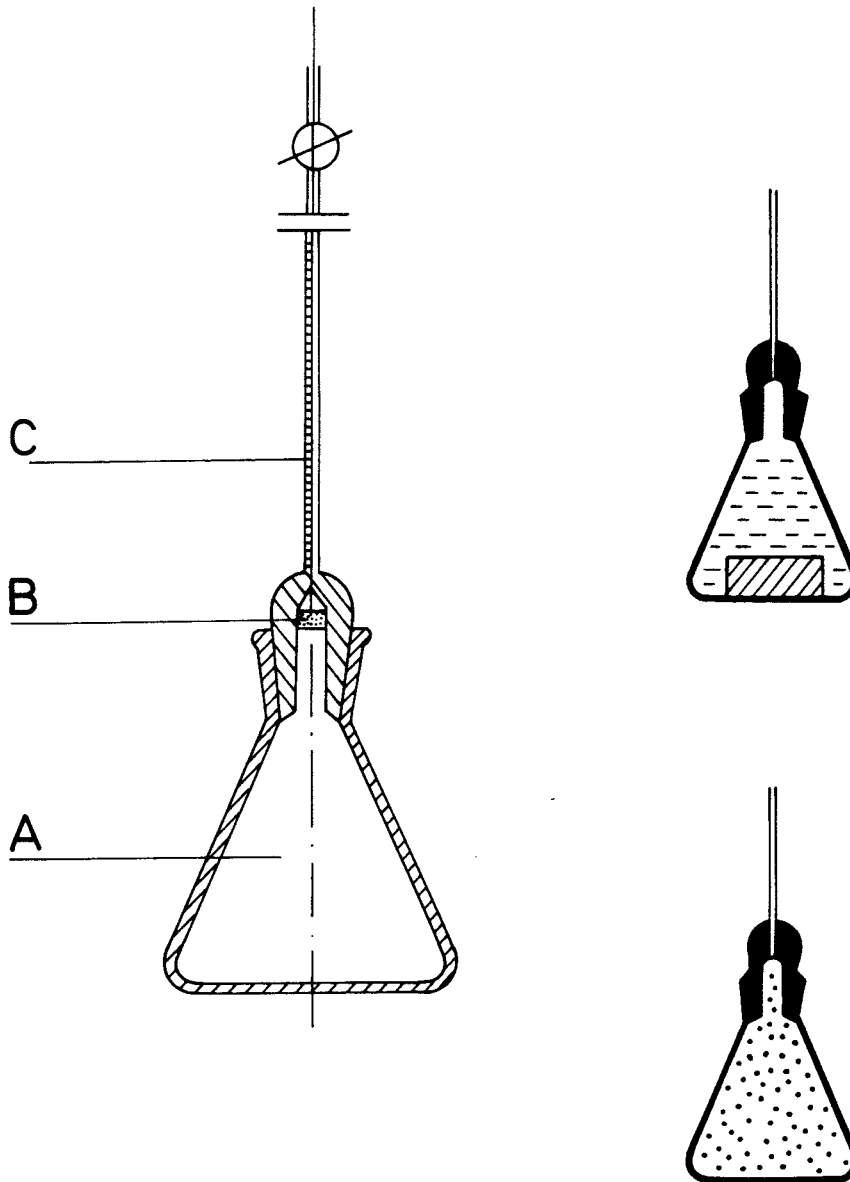


Fig 22. The pycnometer/capillary device. A) 60 cm^3 pycnometer, B) Glass filter, C) Capillary 2.2 mm inner diameter.
 Upper right: Dense clay sample submerged
 Lower right: Appearance after complete dispersion

4.3.5 Test program

Clay samples saturated with distilled water were emplaced in the pycnometer, which contained distilled water in one series and 0.3 M CaCl_2 in a second series, the purpose of the latter being to convert the clay to calcium form, which is expected to cause collapse of the interlamellar water lattice if the initial structure is open and of low density. The main test data are collected in Table 3.

Table 3. Test data

Test no	Pycnometer water	Bulk density, g/cm ³		Pore water mass, g	
		Dense sample		Dense sample	Expanded gel
1	Dist	2.20	4.10	49	
2	Dist	2.05	6.55	49	
3	Dist	2.00	7.40	49	
4	Dist	2.00	7.40	49	
5	Dist	1.80	11.90	49	
6	CaCl_2	2.05	6.55	31	
7	CaCl_2	2.00	7.40	31	
8	CaCl_2	2.00	7.40	31	

4.3.6 Test results

4.3.6.1 **General**

The observation was made that no air emerged from the dense samples, except for a very minute quantity in one of the CaCl_2 tests. Thus, the degree of saturation was equal to or very near to 100 % in the tests.

The net change in volume as interpreted from the motion of the meniscus in the capillary - with due temperature correction - indicated shrinkage in all the tests, the interpretation being specified for each individual test in the subsequent text. The shrinkage was not fully developed until several days had passed after immersing the dense samples in the pycnometer. The recorded volume change was so

large and systematic in the tests that it cannot be explained by irrelevant experimental conditions or errors.

4.3.6.2 Distilled water

The diagram in Fig 23 depicts the recorded volume change of the clay/water system in the five tests, and they can be interpreted in the following specified way.

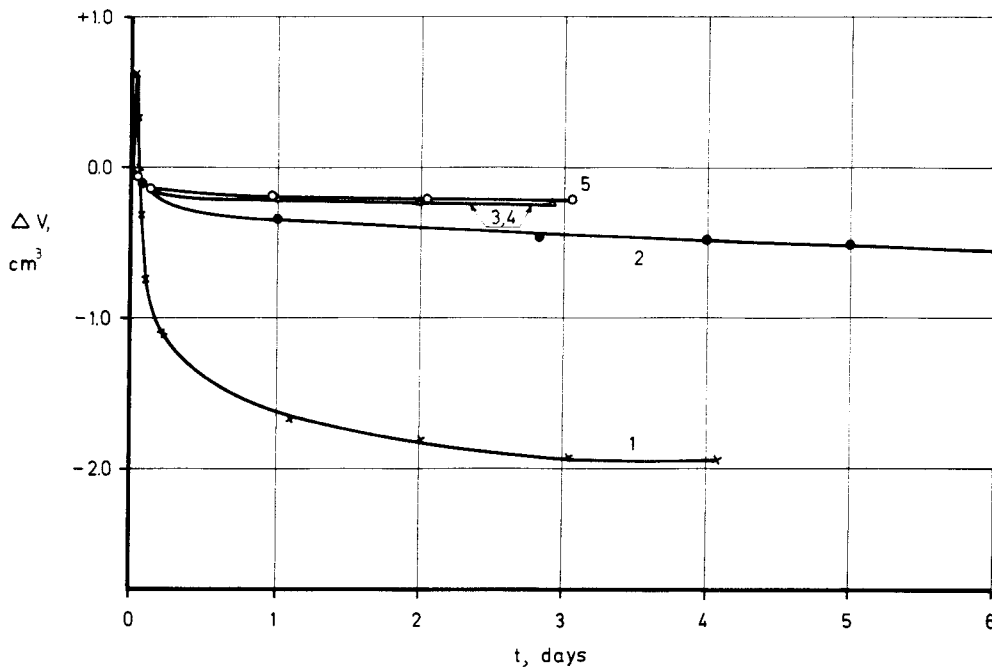


Fig 23. Change in volume of the clay/water systems as a function of time for the clay samples expanded in distilled water

Test no 1, (Distilled water, density of dense sample = 2.20 t/m³)

After a temporary expansion by slightly more than 0.6 cm³, the volume of the clay/water system decreased by 1.94 cm³ from the initial value in 6 days and tended to drop slightly even beyond the 8th day. The expanded gel filled the pycnometer completely and its average density was estimated at slightly higher than 1.3 t/m³. Assuming that all the

water in the dense clay sample was "internal" and had an initial density ρ_i , and that the expanded clay contained only external water with a density of 1.00 g/cm^3 we find that the recorded volume decrease yields $\rho_i = 0.68 \text{ g/cm}^3$. In this particular test there were considerable uncertainties in measuring the volume changes because the initial expansion took place so rapidly. The accuracy of the measurement and therefore of the evaluated water density was low and the test is therefore only valuable from a qualitative point of view.

The initial expansion probably resulted from a competition between adsorption and release of interlamellar water. Thus, 2 and possibly 3 interlamellar hydrate layers of presumably low density grew from the initial monolayer and the associated expansion preceded and superseded the dispersion of the stacks in the first few hours. Later, after completion of the 3-layer hydrates in interlamellar positions in a certain fraction of the clay sample, the dispersion and disappearance of internal water became dominant.

Test no 2 (Distilled water, density of dense sample = 2.05 t/m^3)

The drop in volume of the clay/water system amounted to 0.55 cm^3 in 26 days. The gel appeared to fill the pycnometer almost completely and assuming the expansion to have yielded a homogeneous gel its bulk density would correspond to about 1.3 g/cm^3 . Also in this test there was an initial expansion but it was very much smaller than in Test no 1 and will not be considered here.

Assuming that all the water in the dense clay sample had the same initial density ρ_i and that the net water density ρ^e was equal to that of free water throughout the expanded clay gel, we find for $\rho^e = 1.00 \text{ g/cm}^3$ that $\rho_i = 0.92 \text{ g/cm}^3$. If the more reasonable figures 60 % for the internal water of the dense sample and 3 % for that of the expanded sample are applied and the density ρ^e of external water is taken as 1.00 g/cm^3 , we arrive at $\rho_i = 0.82 \text{ g/cm}^3$.

Test no 3, (Distilled water, density of dense sample = 2.00 t/m^3)

The observed drop in volume of the clay/water system was 0.23 cm^3 in 6 days. The gel filled the pycnometer as completely as in Tests no 1 and 2, and the internal water of the expanded gel was therefore concluded to form approximately the same part of the total water as in the previous test. Taking the fraction of internal water to be 3 % after expansion and the corresponding fraction of the dense sample as 50 %, we find the density of internal water to be $\rho_i = 0.91 \text{ g/cm}^3$.

Test no 4, (Distilled water, density of dense sample = 2.00 t/m^3)

The result of this test appeared to be almost identical to that of Test no 2. Thus, the reduction in volume of the clay/water system was found to be 0.23 cm^3 in 5 days, yielding the same result as in Test no 1, i.e. $\rho_i = 0.91 \text{ g/cm}^3$.

Test no 5, (Distilled water, density of dense sample = 1.80 t/m^3)

According to the diagram in Fig 10 and subsequent corrections, the internal water in the dense sample constituted about 30-50 % of the total water content, while the corresponding percentage of the expanded gel was only a few percent. Taking the content of internal water of the dense sample as 40 % and that of the expanded gel as 3 %, we find the density of the internal water, ρ_i , to be 0.94 g/cm^3 .

4.3.6.3 CaCl_2 solution

Fig 24 shows the volume decrease of the various clay samples in the course of their expansion in CaCl_2 solution.

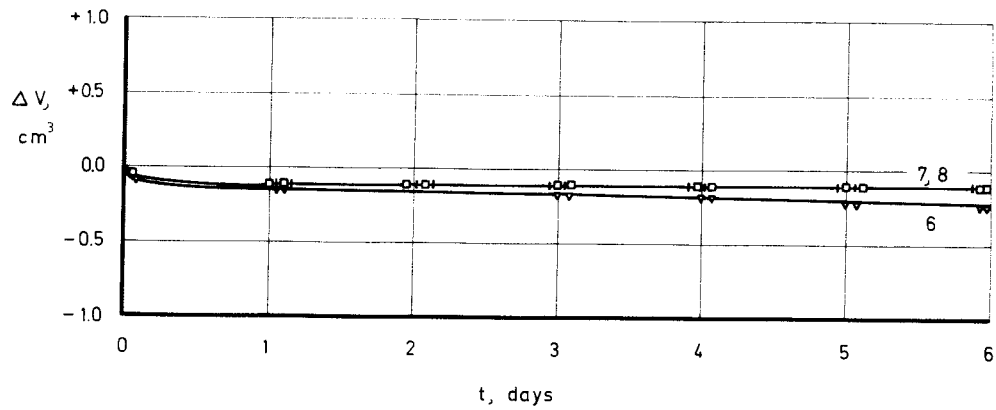


Fig 24. Change in volume of the clay/water systems as a function of time for the clay samples expanded in CaCl_2 solution

Test no 6, (CaCl_2 solution, density of dense sample = 2.05 t/m^3)

The reduction in volume of the clay/water system amounted to 0.25 cm^3 in 6 days. The expansion of the gel, which turned out to be completed in about 25 days, did not proceed to fill the pycnometer and the estimated bulk density of the gel was 1.4 t/m^3 . It appeared as an irregularly shaped mass of large fluffy aggregates. The amount of internal water of the dense sample must have been on the same order as in Test no 2, i.e. about 60 % of the initial 6.55 g but while this particular water phase almost vanished at the expansion in Test no 2 much of it was retained, somewhat reshaped, in the Ca-tests. The introduction of the sample in Ca-rich water must have led to rapid ion exchange associated with the formation of large stacks with much internal water. Assuming that the volume of this water after the expansion had remained unchanged from the initial state or that it had been only slightly reduced, its density must have increased as concluded from the recorded drop in volume of the clay/water system. If the volume of internal water had been reduced to considerably less than that of the initial, dense clay sample, its density may have decreased on the other hand. The critical percentage of internal water of the expanded gel that would imply a higher density than in

the initial clay sample is 13.5 %, and since the actual content is most probably higher than that, it can be assumed that the calcium uptake led to a denser state of the internal water.

Test no 7, (CaCl_2 solution, density of dense sample = 2.00 t/m^3)

The observed drop in volume of the clay/water system was only 0.12 cm^3 , the net bulk density of the expanded gel being estimated at 1.4 g/cm^3 as in the preceding test. Taking the fraction of internal water in the dense sample to be 50 %, the percentage of such water in the expanded gel at which its density becomes higher than in the dense clay sample is 12.3 %. We are therefore led to the same conclusion as previously, i.e. that the Ca uptake gave a denser state of the internal water than in the Na state.

Test no 8, (CaCl_2 solution)

This test gave an almost identical volume decrease as in Test no 7, i.e. $0.12(5) \text{ cm}^3$, which supports the assumption that the accuracy in measuring the volume changes is sufficiently high for the present purpose.

4.4 Discussion

4.4.1 General

The tests offer different explanations of the recorded change in volume of the clay/water systems with respect to the density of the pore water. They will be discussed here with respect to accuracy, influence of the assumed ratio of internal/external water, and the effect of ion exchange from Na to Ca.

4.4.2 Accuracy

The large size of the samples and the very clear change in volume of the clay/water system on dispersion in the de-aired solutions, together with the careful temperature correction, would imply a high accuracy of the measurements. Thus, the accuracy of the volume measurements is estimated at 0.001 cm^3 in all the tests. The total

amount of porewater was calculated from the experimentally determined water content and solid mineral mass, while that of the expanded gel was calculated on the basis of its estimated volume and known amount of solid matter. These quantities were known with an accuracy of $\pm 1\%$ for the dense samples and $\pm 2\%$ for the expanded gels. This allows for an evaluation of the average density of the porewater with an accuracy of $\pm 0.01 - \pm 0.02 \text{ g/cm}^3$ except in the case of Test no 1. However, the accuracy of the calculated density of internal water is entirely dependent on the assumed ratio of internal and external water as discussed in the subsequent chapter.

4.4.3 Influence of the ratio of internal and external water

It is quite clear that while the amount of internal water in the initial, dense clay samples is not critical to the evaluation of its density, the fraction of such water in the expanded state certainly is. There are actually two possible evaluations of the pycnometer measurements, one being that the density ρ_i of the internal water is lower than that of free water and thus of the external porewater (ρ_e), the other being the improbable case that ρ_i is higher than ρ_e . The first-mentioned case yields the mathematical relationship:

$$\rho_w = \frac{\Delta m_{wi}}{\Delta V_{wi} - \Delta V} \quad (3)$$

where $\rho_w = \rho_e = 1 \text{ g/cm}^3$

Δm_{wi} = change in mass of internal water on expansion

ΔV_{wi} = change in volume of internal water on expansion

ΔV = recorded change in volume of the entire clay/water system

We obtain from this relationship the expression:

$$\rho_{wi} = \frac{1}{1 + \frac{(m_w' \cdot p' - m_w'' \cdot p'') 10^{-2}}{\Delta V}} \quad (4)$$

where m_w' = mass of water in the dense sample

p' = percentage of internal water, i.e. water in interlamellar positions

m_w'' = mass of water in the expanded gel

p'' = percentage of internal water in the expanded gel

The second case, implying $\rho_i > \rho_e$ leads to the expression:

$$\rho_{wi} = \frac{1}{\Delta V} \frac{1}{1 - \frac{(m_w'' \cdot p'' - m_w' \cdot p') \cdot 10^{-2}}{\Delta V}} \quad (5)$$

The relationships in Eqs. (4) and (5) are graphically depicted in Fig 25, which demonstrates the importance of the factors m_w'' and p'' . The sensitivity of the parameter p'' is illustrated by the change in ρ_{wi} when p'' increases from 0 to 40 % in Tests no 2 and 5 (Table 4). We see that the evaluated ρ_{wi} -value is not very much affected if we let p'' take the value 0 to 3 %, while it is dramatically altered if p'' exceeds 5-6 %. The figure 3 % that was used in the evaluations is estimated to be very reasonable and it probably represents an upper limit for the fraction of water that is in true interlamellar positions in the very soft gels that expanded in distilled water.

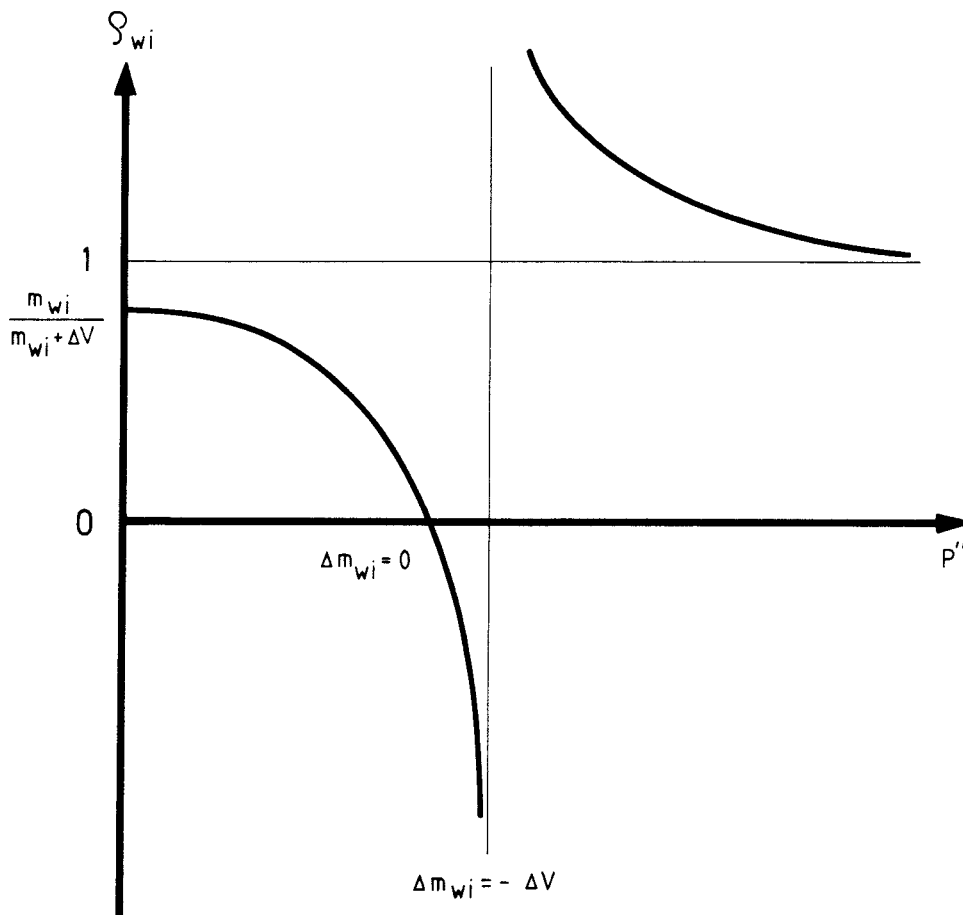


Fig 25. General relationship between the density of internal water and the amount of such water in the non-expanded and expanded states (Eqs. no 4 and 5)

Table 4. Evaluated density of interlamellar water in Na montmorillonite as a function of p'' in Tests no 2 and 5

p'' %	ρ_j , g/cm ³	
	$\rho=2.05$ g/cm ³ ($p'=60$ %)	$\rho=1.80$ g/cm ³ ($p'=40$ %)
0	0.88	0.96
1	0.86	0.95
2	0.84	0.95
3	0.82	0.94
4	0.78	0.93
5	0.73	0.92
6	0.64	0.90
7	0.47	0.86
8	0.02	0.80
9	-6.6	0.63
10	2.33	-2.03
11	1.61	1.50
12	1.40	1.23
20	1.10	1.04
40	1.04	1.01

While Test no 1 gave water density values that are in the same range as those of Forslind's hydration model, we find Tests no 3, 4 and 5 to yield values that agree well with those reinterpreted from Low & Anderson's results (p 24), i.e. slightly higher than 0.9 g/cm³. Test no 2 gave a density of the interlamellar water that is intermediate to Forslind's range and that of the values reinterpreted from Low & Anderson's study. In general these values and the authors' experimental results are in agreement also with Sposito's idea of an ice-like structure of the first interlamellar hydrate layer.

Qualitatively, we take as a working hypothesis that water molecules in interlamellar positions in Na montmorillonite are arranged in a strained, ice-like lattice form. Forslind's model is not perfectly applicable but it can be taken as a prototype which is preliminarily adopted here. Naturally, it may well be subjected to alteration or may even be abandoned in the course of the ongoing research.

Theoretically, it is possible that the outer surfaces of montmorillonite stacks, which become numerous in the course of the expansion, become hydrated with water in dense layering. If the density is taken to be 1.05 t/m^3 of a monolayer, it would mean that the aforementioned density values of water in interlamellar positions is underestimated by 10-20 %. The influence of such density anomalies is thus not very significant but it requires attention in more detailed, forthcoming analyses.

4.4.4 Influence of exchange from Na to Ca

The tests in which the dense clay was dispersed in CaCl_2 solution do not offer a way of determining the density of internal water in the initial dense clay samples or in the expanded gels, while it is possible to conclude which of them had the highest density if the relative amounts of internal and external water can be estimated. The critical point is the microstructural arrangement of flakes in the expanded state in the CaCl_2 solution. No detailed microstructural data are available from which quantitative determinations can be made, but the common concept of limited spontaneous dispersion of Ca montmorillonite suggests that the number of associated flakes in dispersed Ca montmorillonite is many times that of Na montmorillonite (Fig 26). The conclusion from the tests with CaCl_2 solution that the amount of internal water was higher after expansion than in the initial Na clay samples is therefore reasonable. It must be realized, however, that only 2 hydrate layers are hosted in interlamellar voids, while 3 layers may have been present in some of the dense Na montmorillonite samples. With the present limited knowledge of the microstructural features of dispersed Ca montmorillonite, no safe conclusions can be drawn as to the organization and density of its interlamellar water.

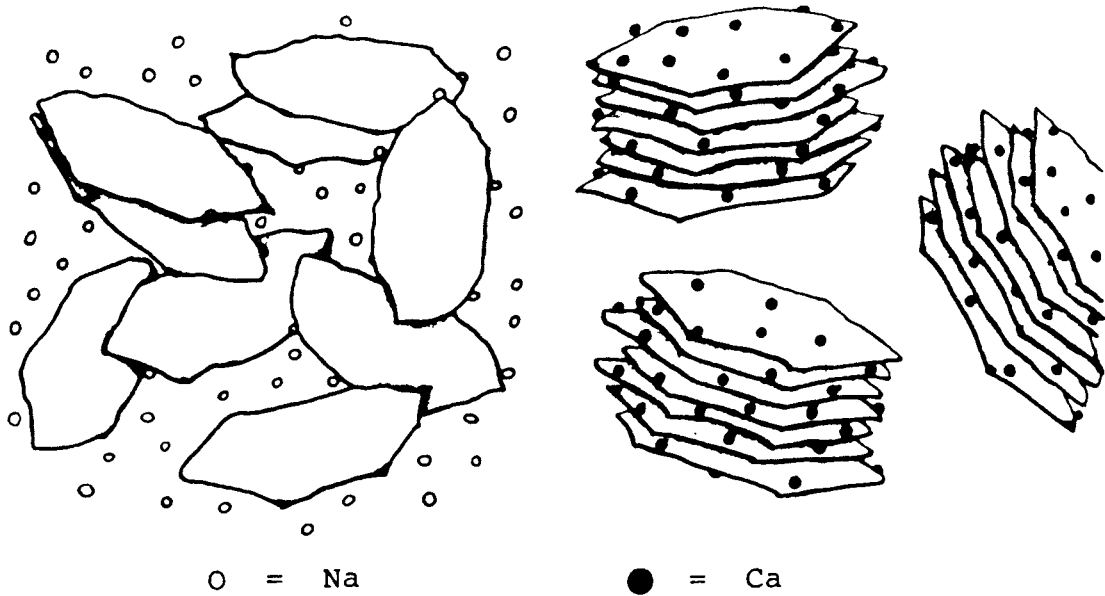


Fig 26. Left: Irregular type of particle association in Na-saturated montmorillonite clay. Right: Domain-type arrangement of crystallites in Ca-saturated montmorillonite (After Fahn)

5 CONCLUSIONS

The microstructural arrangement of the thin crystal flakes is concluded to be of great importance in the evaluation of the organization and physical state of the porewater in montmorillonite clay. This arrangement has been found to be very much dependent on the bulk density. For Na montmorillonite, the HVEM study and various investigations of resin-embedded clay yield the schematic models in Fig 27, the version for dense clay characteristically containing a certain, rather small number of continuous voids and local pores which are more or less continuous and in which the water is poorly organized because of imperfect orientation of neighboring crystals. Here, and in the large pores, electrical double-layers determine the equilibrium distance between the "quasicrystals" of regularly stacked montmorillonite flakes, which are assumed to be separated by well orga-

nized interlamellar water of low density, possibly represented by Forslind's model. This speaks in favor of the Edelman/Favejee crystal structure provided that the temperature is sufficiently low. A necessary implication in applying this model is that hydrogen bonds are largely responsible for the stability and physical properties of the interlamellar water, while electrostatic forces may be more important for the water associated with the mineral surfaces that are exposed in the voids. The ordering of water molecules to form open lattices is assumed to be produced only in interlamellar positions when the adjacent flakes are oriented so that the directions of their crystallographic axes coincide. The ordering influence on adjacent water molecules at free "external" surfaces of the stacks is too weak to organize the water as in the interlamellar space and largely random grouping is expected here.

In Na montmorillonite gels which are allowed to swell in electrolyte-poor water, the quasicrystals expand to hold 2-3 interlamellar hydrate layers which breaks them up in thin fragments due to mechanical stresses which are set up in the expansion process. At the freshly formed free surfaces, electrical double-layers are developed in which the water is probably not organized. The ultimate state is a very soft gel with very thin stacks and almost all the porewater being unaffected by the minerals.



Fig 27. Upper: Dense Na montmorillonite clay. A) Large pore, B) Small void with external water, C) Stack or quasicrystal with organized interlamellar water, D) Interface between stacks. Lower: Expanded Na montmorillonite gel with very thin stacks and practically only external water

One consequence of this hypothetical microstructure of dense montmorillonite clay may be that chemical reactions, such as ion exchange and charge change by tetrahedral release of Si and uptake of Al, start at the interface between the stacks and in their shallow parts. Thus, the formation of mixed layer minerals would not result from a randomly or uniformly distributed layer alteration but may well

result from attacks at the interface of neighboring stacks. Thus, the initial points of chemical attack are very probably determined by the microstructural features. This first attack may, in turn, create mechanical stresses that break these larger homogeneous units and expose new surfaces to chemical attack. We may thus have obtained an explanation of the phenomenon that illite layers in mixed layer bentonites do not occur in large continuous series but are regularly or irregularly distributed in the stacks.

From a practical engineering point of view there are several important consequences of this tentative water structure model:

- * A significant part of the porewater has a higher, elastic compressibility than that of free water
- * The ordering of interlamellar water implies that it has plastic properties, i.e. there is a threshold shear stress that must be exceeded before significant permanent strain is developed. This property would also be characteristic of the stacks, which therefore deserve to be termed quasicrystals
- * Since the fraction of internal water is not significantly reduced when the bulk density drops from about 2 t/m^3 to $1.6\text{-}1.8 \text{ t/m}^3$ the rheological properties are only moderately altered on such a reduction in density. However, it is expected to produce a significant change in interconnectivity of pervious passages and therefore in bulk permeability, as has been verified in numerous experiments. The expansion associated with the drop in density also means that the pores and interface zones between adjacent stacks become enlarged which also makes the clay/water system more pervious. Such widening means that electrical double-layers become largely decisive of the swelling properties when the density is reduced to less than $1.9\text{-}2.0 \text{ t/m}^3$, which is beautifully illustrated by Fig 28. It demonstrates that the porewater chemistry does not affect the swelling pressure at higher bulk densities than about 2.0 t/m^3 .

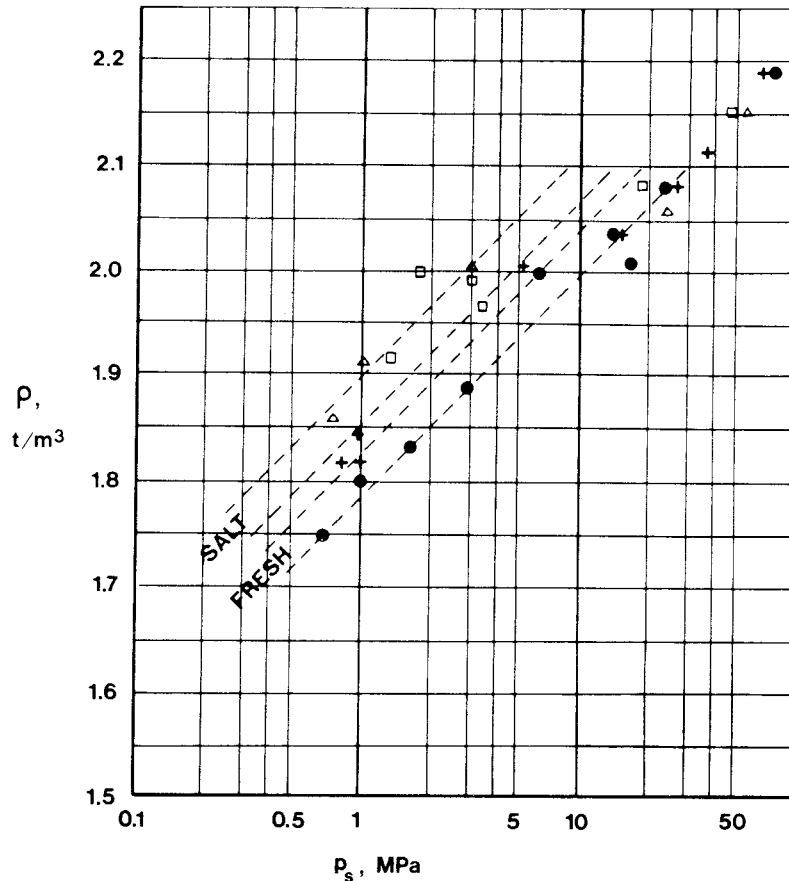


Fig 28. Recorded swelling pressure of MX-80 bentonite at 20° C.
 Notes: + artificial groundwater, ● distilled water, Δ 0.6 M NaCl solution, □ 0.3 M CaCl₂ solution

6 RECOMMENDATIONS FOR FURTHER WORK

Naturally, the tentative model of organization of water in Na montmorillonite that has been derived needs to be further tested. Since it is related to the Edelman/Favejee crystal structure it is recommended that the research comprises physico/chemical analyses and relevant NMR investigations. The following program is suggested:

- * Extension of the test series concerning the porewater density with other cations
- * Shear tests of clay specimens prepared so that virtually all stacks are aligned. Shear takes place at different normal pressures under undrained conditions and with pore pressure measurement

- * MAS/NMR technique focussing on ^{29}Si and ^{17}O in tetrahedral positions to find out expected changes related to heat-induced EF/HEW translation

7 ACKNOWLEDGEMENTS

The authors are greatly indebted to Professor Bernard Jouffrey who is the head of the CNRS Laboratoire d'Optique Electronique in Toulouse, France, for putting his staff and microscope resources to the authors' disposal for part of the study.

Also, they wish to thank Harald Hökmark and Lennart Börgesson, members of the SGAB staff in Lund, for many valuable discussions and suggestions.

Finally, they like to express their sincere gratitude to Jeanette Stenelo who was responsible for transforming the awkward manuscript to a readable form, and to Birgitta Hellström for her carefully made drawings.

8 REFERENCES

- 1 Forslind, E., & Jacobsson, A. Water, a Comprehensive Treatise (Ed. Franks) Ch. 4. Clay-water systems, Plenum, New York, 1972
- 2 Cowley, J.M. & Goswami, A. Electron Diffraction Patterns from Montmorillonite. Acta Cryst. Vol. 14, 1961 (p. 1071-1079)
- 3 Mering, J. & Oberlin, A. The Smectites. In: J.A. Gard (Ed.) The Electron-Optical Investigations of Clays. Mineral. Soc. Monogr. Vol. 3, 1971 (pp 193-229)
- 4 Pusch, R. Stability of Bentonite Gels in Crystalline Rock - Physical Aspects. SKBF/KBS Technical Report 83-04, 1983
- 5 Pusch, R. A Technique for Investigation of Clay Microstructure. J. Microscopie, Vol. 6, 1967
- 6 Tessier, D. Etude Experimentale de l'Organisation des Materiaux Argilleux, INRA, (361 pp)
- 7 Grabowska-Olszewska, B., Osipov, V. & Sokolov, V. Atlas of the Microstructure of Clay Soils. Panstwowe Wydawnictwo Naukowe, Warszawa, 1984
- 8 Smart, P. & Tovey, N.K. Electron Microscopy of Soils and Sediments: examples. Clarendon Press, Oxford, 1981
- 9 Bennett, R.H. Clay Fabric and Geotechnical Properties of Selected Submarine Sediment Cores from the Mississippi Delta. U.S. Dep. of Commerce. Nat. Oceanic and Atmosph. Adm. NOAA, Prof. Paper 9, 1977
- 10 Karlsson, R. & Pusch, R. Shear Strength Parameters and Microstructure Characteristics of a Quick Clay of Extremely High Water Content. Proc. Geot. Conf. Oslo, Vol. 1/7, 1967

- 11 Pusch, R. Clay Microstructure. Document D8:1970, Nat. Swedish Building Res. Council, 1970
- 12 Pusch, R. Microstructural Features of Pre-quaternary Clays. Acta Universitatis Stockholmiensis, Stockholm Contributions in Geology, Vol. XXIV, Almqvist & Wiksell, 1971
- 13 Sposito, G. & Prost, R. Structure of Water Adsorbed on Smectites. Chemical Reviews, Vol. 82, No. 6, 1982 (pp 553-573)
- 14 Pusch, R., Eriksen, T.E. & Jacobsson. A. Ion/water Migration Phenomena in Dense Bentonites. In (Ed) Lutze, W. Scientific Basis for Nuclear Waste Management. Elsevier Publ. Co., 1982 (p. 649)
- 15 Low, P.F. Nature and Properties of Water in Montmorillonite-Water Systems. Soil Science Soc. Am. J., Vol. 45, 1979 (p 651)
- 16 Musslehi, M., Lambrosa, A. & Marinsky, J.A. The Interaction of Bentonite and Glass with Aqueous Media. SKBF/KBS Technical Report 83-33, Stockholm 1983
- 17 Pusch, R. Mineral-Water Interactions and Their Influence on the Physical Behavior of Highly Compacted Na Bentonite. Can. Geot. J. Vol. 19, No 3, 1982 (pp 381-387)
- 18 Tardy, Y., Lesniak, P., Duplay, J. & Prost, R. Energies d'Hydratation des Argiles. Application a l'Hectorite. Bull. Mineral. Vol. 103, 1980 (pp. 217-223)
- 19 Anderson, D.M., & Low, P.F. The Density of Water Adsorbed by Lithium-, Sodium-, and Potassium Bentonite. Soil Sci. Soc. Am. Proc. Vol. 22, 1958 (pp 99-103)
- 20 Anderson, D.M., Leaming, G.F. & Sposito, G. Volume Changes of a Thixotropic, Sodium Bentonite Suspension during Sol-Gel-Sol Transition. Science, Vol. 141, No 3585, 1963 (pp. 1040-1041)

- 21 Low, P.F. Nature and Properties of Water in Montmorillonite-Water Systems. Soil Sci. Soc. Am. J. Vol. 43, No. 5, 1979 (pp 651-658)
- 22 Knutsson, S. Buffer Mass Test - Thermal Calculations for the High Temperature Test. Stripa Project, SKBF/KBS Internal Report 83-03, 1983
- 23 Pusch, R. Identification of Na Smectite Hydration by use of "Humid Cell" High Voltage Microscopy (In press)
- 24 Güven, N. Electron-Optical Investigations on Montmorillonites. I. Cheto, Camp-Berteaux and Wyoming Montmorillonites. Clays and Clay Minerals, Vol. 22, 1974 (pp 155-165)
- 25 Cebula, D.J. & Thomas, R.K. Small Angle Neutron Scattering from Dilute Aqueous Dispersions of Clay. J. Chem. Soc. Faraday Trans. Vol. 16, 1980 (pp 314-321)

List of SKB reports

Annual Reports

1977-78

TR 121

KBS Technical Reports 1 – 120.

Summaries. Stockholm, May 1979.

1979

TR 79-28

The KBS Annual Report 1979.

KBS Technical Reports 79-01 – 79-27.
Summaries. Stockholm, March 1980.

1980

TR 80-26

The KBS Annual Report 1980.

KBS Technical Reports 80-01 – 80-25.
Summaries. Stockholm, March 1981.

1981

TR 81-17

The KBS Annual Report 1981.

KBS Technical Reports 81-01 – 81-16.
Summaries. Stockholm, April 1982.

1982

TR 82-28

The KBS Annual Report 1982.

KBS Technical Reports 82-01 – 82-27.
Summaries. Stockholm, July 1983.

1983

TR 83-77

The KBS Annual Report 1983.

KBS Technical Reports 83-01 – 83-76
Summaries. Stockholm, June 1984.

1984

TR 85-01

Annual Research and Development Report 1984

Including Summaries of Technical Reports Issued during 1984. (Technical Reports 84-01-84-19)
Stockholm June 1985.

1985

TR 85-20

Annual Research and Development Report 1985

Including Summaries of Technical Reports Issued during 1985. (Technical Reports 85-01-85-19)
Stockholm May 1986.

Technical Reports

1986

TR 86-01

I: An analogue validation study of natural radionuclide migration in crystalline rock using uranium-series disequilibrium studies

II: A comparison of neutron activation and alpha spectroscopy analyses of thorium in crystalline rocks

JAT Smellie, Swedish Geological Co, A B MacKenzie and RD Scott, Scottish Universities Research Reactor Centre
February 1986

TR 86-02

Formation and transport of americium pseudocolloids in aqueous systems

U Olofsson
Chalmers University of Technology, Gothenburg, Sweden
B Allard
University of Linköping, Sweden
March 26, 1986

TR 86-03

Redox chemistry of deep groundwaters in Sweden

D Kirk Nordstrom
US Geological Survey, Menlo Park, USA
Ignasi Puigdomenech
Royal Institute of Technology, Stockholm, Sweden
April 1, 1986

TR 86-04

Hydrogen production in alpha-irradiated bentonite

Trygve Eriksen
Royal Institute of Technology, Stockholm, Sweden
Hilbert Christensen
Studsvik Energiteknik AB, Nyköping, Sweden
Erling Bjergbakke
Risø National Laboratory, Roskilde, Denmark
March 1986

TR 86-05

Preliminary investigations of fracture zones in the Brändan area, Finnsjön study site

Kaj Ahlborn, Peter Andersson, Lennart Ekman, Erik Gustafsson, John Smellie, Swedish Geological Co, Uppsala
Eva-Lena Tullborg, Swedish Geological Co, Göteborg
February 1986

TR 86-06

Geological and tectonic description of the Klipperås study site

Andrzej Olkiewicz
Vladislav Stejskal
Swedish Geological Company
Uppsala, October, 1986

TR 86-07

Geophysical investigations at the Klipperås study site

Stefan Sehlstedt
Leif Stenberg
Swedish Geological Company
Luleå, July 1986

TR 86-08

Hydrogeological investigations at the Klipperås study site

Bengt Gentschein
Swedish Geological Company
Uppsala, June 1986

TR 86-09

Geophysical laboratory investigations on core samples from the Klipperås study site

Leif Stenberg
Swedish Geological Company
Luleå, July 1986

TR 86-10

Fissure fillings from the Klipperås study site

Eva-Lena Tullborg
Swedish Geological Company
Göteborg, June 1986

TR 86-11

Hydraulic fracturing rock stress measurements in borehole Gi-1, Gideå Study Site, Sweden

Bjarni Bjarnason and Ove Stephansson
Division of Rock Mechanics,
Luleå University of Technology, Sweden
April 1986

TR 86-12

PLAN 86— Costs for management of the radioactive waste from nuclear power production

Swedish Nuclear Fuel and Waste Management Co
June 1986

TR 86-13

Radionuclide transport in fast channels in crystalline rock

Anders Rasmuson, Ivars Neretnieks
Department of Chemical Engineering
Royal Institute of Technology, Stockholm
March 1985

TR 86-14

Migration of fission products and actinides in compacted bentonite

Börje Torstenfelt
Department of Nuclear Chemistry, Chalmers
University of Technology, Göteborg
Bert Allard
Department of water in environment and society, Linköping university, Linköping
April 24, 1986

TR 86-15

Biosphere data base revision

Ulla Bergström, Karin Andersson, Björn Sundblad, Studsvik Energiteknik AB,
Nyköping
December 1985

TR 86-16

**Site investigation
Equipment for geological, geophysical, hydrogeological and hydrochemical characterization**

Karl-Erik Almén, SKB, Stockholm
Olle Andersson, IPA-Konsult AB, Oskarshamn
Bengt Fridh, Bengt-Erik Johansson,
Mikael Sehlstedt, Swedish Geological Co, Malå
Erik Gustafsson, Kenth Hansson, Olle Olsson,
Swedish Geological Co, Uppsala
Göran Nilsson, Swedish Geological Co, Luleå
Karin Axelsen, Peter Wikberg, Royal Institute of Technology, Stockholm
November 1986

TR 86-17

Analysis of groundwater from deep boreholes in Klipperås

Sif Laurent
IVL, Swedish Environmental
Research Institute
Stockholm, 1986-09-22

TR 86-18

Technology and costs for decommissioning the Swedish nuclear power plants.

Swedish Nuclear Fuel and Waste Management Co
May 1986

TR 86-19

Correlation between tectonic lineaments and permeability values of crystalline bedrock in the Gideå area

Lars O Ericsson, Bo Ronge
VIAK AB, Vällingby
November 1986

TR 86-20

A Preliminary Structural Analysis of the Pattern of Post-Glacial Faults in Northern Sweden

Christopher Talbot, Uppsala University
October 1986

TR 86-21

Steady-State Flow in a Rock Mass Intersected by Permeable Fracture Zones. Calculations on Case 2 with the GWHRT-code within Level 1 of the HYDROCOIN Project.

Björn Lindbom, KEMAKTA Consultants Co,
Stockholm
December 1986

TR 86-22

Description of Hydrogeological Data in SKBs Database Geotab

Bengt Gentschein, Swedish Geological Co,
Uppsala
December 1986

TR 86-23

Settlement of Canisters with Smectite Clay Envelopes in Deposition Holes

Roland Pusch
Swedish Geological Co
December 1986

TR 86-24

Migration of Thorium, Uranium, Radium and Cs—137 in till Soils and their Uptake in Organic Matter and Peat

Ove Landström, Björn Sundblad
Studsvik Energiteknik AB
October 1986